IT9600105

Associazione EURATOM-ENEA sulla Fusione

LASER INDUCED FLUORESCENCE SPECTROSCOPY FOR FTU

T.P. HUGHES*
ENEA- Dipartimento Energia
Centro Ricerche di Frascati, Roma

Permanent address: JET Joint Undertaking, Abingdon, Oxon OX14 3EA (UK)

RT/ERG/FUS/94/27

VOL 27 N. U 6

ENTE PER LE NUOVE TECNOLOGIE,
L'ENERGIA E L'AMBIENTE

Associazione EURATOM-ENEA sulla Fusione

LASER INDUCED FLUORESCENCE SPECTROSCOPY FOR FTU

T.P. HUGHES*
ENEA- Dipartimento Energia
Centro Ricerche di Frascati, Roma

Permanent address: JET Joint Undertaking, Abingdon, Oxon OX14 3EA (UK)

RT/ERG/FUS/94/27

Paper received in July 1995

This report has been prepared and distributed by: Servizio Edizioni Scientifiche - ENEA Centro Ricerche Frascati, C.P. 65 - 00044 Frascati, Rome, Italy

The technical and scientific contents of these reports express the opinion of the authors but not necessarily those of ENEA.

SUMMARY

Laser induced fluorescence spectroscopy (LIFS) is based on the absorption of a short pulse of tuned laser light by a group of atoms and the observation of the resulting fluorescence radiation from the excited state. Because the excitation is resonant it is very efficient, and the fluorescence can be many times brighter than the normal spontaneous emission, so low number densities of the selected atoms can be detected and measured. Good spatial resolution can be achieved by using a narrow laser beam. If the laser is sufficiently monochromatic, and it can be tuned over the absorption line profile of the selected atoms, information can also be obtained about the velocities of the atoms from the Doppler effect which can broaden and shift the line. In this report two topics are examined in detail. The first is the effect of high laser irradiance, which can cause "power broadening" of the apparent absorption line profile. The second is the effect of the high magnetic field in FTU. Detailed calculations are given for LIFS of neutral iron and molybdenum atoms, including the Zeeman effect, and the implementation of LIFS for these atoms on FTU is discussed.

RIASSUNTO

La spettroscopia fatta per mezzo di fluorescenza indotta da laser (LIF) è basata sull'assorbimento di un breve impulso di luce laser accordata su una transizione atomica di un gruppo do atomi e la osservazione della risultante radiazione di fluorescenza emessa a causa del decadimento del livello eccitato. Poiché la eccitazione è risonante, essa è molto efficiente, e la fluorescenza può essere molte volte piú intensa della normale emissione spontanea, in tal modo è possibile misurare radiazione proveniente da atomi presenti a bassa densità. Se il laser è sufficentemente monocromatico e può essere accordato sul profilo di assorbimento degli atomi selezionati, si può misurare anche la distribuzione in velocità degli atomi per mezzo dell'effetto Doppler che sposta ed allarga la riga di assorbimento. In questo report nell'ambito nella attività LIF per FTU due argomenti vengono esaminati in dettaglio. Il primo è l'effetto della alta potenza del laser incidente che può causare un "power broadening" (cioè un allargamento) del profilo di assorbimento della riga. Il secondo è l'effetto dell'alto campo magnetico, presente in FTU, sulla LIF. Calcoli dettagliati sono presentati per la LIF su atomi neutri di Ferro e Molibdeno in riferimento alle misure condotte in laboratorio.

Preface

Laser induced fluorescence spectroscopy (LIFS) is based on the absorption of a short pulse of tuned laser light by a group of atoms and the observation of the resulting fluorescence radiation from the excited state. Because the excitation is resonant it is very efficient, and the fluorescence can be many times brighter than the normal spontaneous emission, so low number densities of the selected atoms can be detected and measured. Good spatial resolution can be achieved by using a narrow laser beam. If the laser is sufficiently monochromatic, and it can be tuned over the absorption line profile of the selected atoms, information can also be obtained about the velocities of the atoms from the Doppler effect which can broaden and shift the line.

LIFS has been shown to provide valuable diagnostic information about impurity atom densities and fluxes in the cool edge region of tokamaks and other plasma machines. For example, the technique has enabled measurements to be made of the density of neutral iron atoms near a stainless steel limiter in the small ISX-B tokamak at Oak Ridge National Laboratory (ORNL) with a detection limit of 10^{12} to 10^{13} m^{-3} (Scheer [1983]). Measurements of neutral iron atoms were also made near the wall of the Heliotron E device by Oda et al. [1984]. On Textor at Julich Fe I density measurements of about 4×10^{15} m^{-3} were made which, when combined with estimates of velocities, gave neutral iron atom flux measurements of order 10^{19} m^{-2} s^{-1} (Bay and Schweer [1984]).

At ENEA, extensive preparatory work has been done by G. Gatti with the intention of using LIFS as an edge plasma diagnostic on the FTU tokamak. The aim is to measure densities and, if possible, velocities, and hence the fluxes of neutral iron and molybdenum atoms emitted from plasma limiters in FTU. On the basis of emission spectroscopic observations (Condrea et al. [1992], McNeill et al. [1992]) the Fe I density in the edge plasma near a limiter has been estimated to be about 4×10^{15} m^{-3}. Near the molybdenum limiter the Mo I density may be somewhat lower because of the larger limiter area. As a preliminary test a tunable, excimer-laser-pumped dye laser at ENEA has been successfully used by M. Borra [1993] to determine the density of neutral iron atoms near a stainless steel electrode bombarded by argon ions in a 1.1 keV discharge. Calculations by Borra, based on this work and on the emission spectroscopy on FTU predict that it will be possible to obtain satisfactory measurements of iron atom densities in the edge region of FTU using LIFS.

In this report two topics are examined in detail. The first is the effect of high laser irradiance, which can cause "power broadening" of the apparent absorption line profile. The second is the effect of the high magnetic field in FTU. Detailed calculations are given for LIFS of neutral iron and molybdenum atoms, including the Zeeman effect, and the implementation of LIFS for these atoms on FTU is discussed.

The theory of LIFS leads to expressions for the number of fluorescence photons produced. Using atomic parameters for the transitions of interest in Fe I and Mo I given in Table I we find that a very intense short laser pulse should cause up to about one fifth of the Fe atoms, or one third of the Mo atoms, to fluoresce, and a longer high power pulse could increase the proportions to three quarters. For a real laser pulse a more detailed treatment is required.

Power broadening, which is also known as saturation broadening, arises because the fluorescence intensity is not a linear function of the laser output power, but approaches a maximum (i.e. saturates) as the power is increased. In most practical cases the effect is not easily calculated. The mode structure of the laser radiation further complicates the theory and deserves further study. Borra [1] has reported clear evidence of power broadening in LIFS experiments at ENEA using sputtered Fe I atoms. The measurements on Fe I at ENEA will be extended, and measurements with Mo I will also be possible. For LIFS experiments designed to study Doppler modified absorption line profiles, we must ensure that power broadening does not distort the profile. The best way to determine the maximum allowable laser irradiance in a given situation is by experimental tests.

The strong magnetic field of order 10 Tesla in FTU can cause significant Zeeman splitting of degenerate atomic energy levels into separate magnetic states. For an atom with LS coupling in weak fields, the change in energy of an atomic state with magnetic quantum number M in a magnetic field B Tesla, from the unperturbed energy, is given by

$$\Delta W = 9.27 \times 10^{-24} M g_L B \quad \text{J}$$

where g_L is the Landé factor for the level. Transitions between the magnetic states of two levels are only allowed if ΔM, the change in M, is equal to 1 or 0. The polarization of the radiation emitted depends on which of these conditions is obeyed: for emission perpendicular to the magnetic field, if ΔM=0 the emission is "π" polarized, with the electric field parallel to B, while if ΔM=±1, the emission is "σ" polarized, with the electric field perpendicular to B.

The emission spectrum due to transitions between two energy levels will consist of the contributions from all the allowed transitions between the magnetic states. If the upper and lower states have different Landé factors, the emission spectrum will consist of components from all the allowed transitions, with wavelength shifts given by

$$\Delta\lambda = 4.67 \times 10^{-5} \lambda^2 \left(\mathrm{M}_1 g_{L1} - \mathrm{M}_2 g_{L2}\right) B \quad \text{pm}$$

where λ is in nm and B in Tesla. If the upper and lower states have the same Landé factors, the emission spectrum will consist of only three lines. The π component, which contains all the ΔM = 0 transitions, will be unshifted. The two σ components, one containing all the ΔM=+1 and the other all the -1 transitions, will be shifted equally to higher and lower frequencies. The relative intensities of the Zeeman components may be calculated assuming equal populations of the magnetic states of the excited level. The intensities depend on the direction of observation, relative to that of the magnetic field.

For Fe I atoms the ground term is a^5D, and absorption to y^5D^0 is suitable for LIFS with laser wavelengths near 300 nm. If the populations of the levels of the ground term with J=0,1,2,3,4 are n_J, their ratios may be estimated from the Boltzmann relationship, using known energy level spacings and degeneracies g_J, if we assume an excitation temperature T. Taking T=1000 K we find that about 57% of the atoms will be in the lowest (J=4) level. The strongest

absorption line, and the most suitable for LIFS excitation, is $a^5D_4 - y^5D_0^4$ at 302.064 nm, for which the Zeeman pattern is shown in Figure 4. Nearby lines in this multiplet are much weaker, and are sufficiently well separated from the strongest line to be normally well resolved, but their Zeeman splitting can be significant (Fig. 5).

The Fe I fluorescence can conveniently be observed in the decay from y^5D^0 to a^5F. Assuming that the J=4 level is selectively pumped by the laser, the strongest line in this multiplet will be $y^5D_4^0$ to a^5F_5 at 382.0425 nm. Competing lines will not normally be detected.

For the Fe I absorption line at 302.06 nm the Zeeman pattern is degenerate (Fig. 4). There is a single unshifted π polarized component so it is convenient to use π polarized laser light. For the fluorescence line at 382.04 nm the Zeeman pattern is more complex with nine π and eighteen σ components (Fig. 6). The fluorescence signal must be detected in the presence of noise, which in a plasma is dominated by continuum radiation, so the π polarized emission, which is contained in a much narrower bandwidth than the σ, should give a better signal-to-noise ratio. The π polarized detector filter bandwidth need be no more than about 270 pm, but in practice is usually wider than this.

With a very short laser pulse, if the total number density of Fe I atoms in the ground term is n_0, then the upper limit to the total, time integrated number of fluorescence photons collected from volume V in π polarization in a detector solid angle $d\Omega$ is found to be

$$N_F = 4.1 \times 10^{-2} n_0 \frac{V d\Omega}{4\pi},$$

allowing for the populations of the lower fine structure levels and the polarization of the emission. A full numerical calculation is needed for a real laser pulse shape, but this expression also gives approximately the correct value of N_F for a 10 ns laser pulse with a laser irradiance per pm of bandwidth of 330 W cm^{-2}.

The velocity distributions of a number of different atoms sputtered from solid surfaces by various high energy ions have been measured by several authors using LIFS (see Bay [1987]). In general, the velocity distributions normal to the surface rise from zero at V=0 to a maximum at V somewhere between 1 and 5 km s^{-1}, and then fall approximately exponentially at higher velocities. The FWHM of the distribution is typically 2 to 10 km s^{-1}. Broadly similar distributions may be expected in the edge plasma of a tokamak. The corresponding wavelength displacements due to the Doppler effect are small compared to the separations of adjacent spectral lines in Fe I. Using a tunable laser with a narrow bandwidth of about 1 pm (achieved with an etalon in the cavity) and a high pulse repetition rate it should be possible to measure the Doppler profile and hence the velocity distribution of sputtered atoms by scanning the laser wavelength through the absorption line profile during a sequence of pulses. Because of the inhomogeneous Doppler broadening, only a fraction of the ground state atoms will be excited at a given setting of the laser wavelength, so the number of fluorescence photons collected per laser pulse will be smaller than that given for a broad band laser. For these measurements it is clearly important to avoid power broadening of the absorption line profile.

For Mo I atoms a survey of absorption lines and subsequent fluorescence lines has identified two feasible LIFS schemes (Table I). The large separation of the fine structure levels of the z^5P^o term means that there will be no interference between the two schemes. The Zeeman patterns for the absorption lines have been calculated (Figs. 7 and 9). The total width of the π polarized pattern in a field of 10 T is ±56 pm for Scheme (a) and ±18 pm for Scheme (b). For the fluorescence lines (Figs. 8 and 10) the spreads of the π patterns at 10 T are ±93 pm for Scheme (a) and ±47 pm for Scheme (b). The σ fluorescence patterns have spreads at 10 T of ±330 pm for Scheme (a) and ±310 pm for Scheme (b). A detector filter bandwidth (FWHM) of 2 nm (less at lower magnetic fields) should be adequate.

In contrast to the Fe I case, where the π polarized absorption line has only a single component, the Mo I absorption lines are split into 5 or 6 Zeeman components separated, in a field of 10 T, by intervals of 18 pm for Scheme (a) and 9 pm for Scheme (b), which are more than the usual laser bandwidth. When the laser wavelength is scanned across the Zeeman pattern each Zeeman component will be excited in turn, and each will be affected by the Doppler broadening and shift. Thus, in contrast to the degenerate Fe I case, if the absorption line Doppler profile of Mo I is to be measured in FTU, the Zeeman effect must be allowed for.

In Scheme (a) for Mo I there is unfortunately no absorption at the unshifted wavelength in a magnetic field. Provided the magnetic field does not change during the scan, each of the absorption line Zeeman components will have a similar Doppler modified profile, and the signal obtained by collected the emission in all the fluorescence components will give each profile in turn. However, any significant variation in the local magnetic field over the emitting volume, or during the laser scan, will distort the apparent Doppler profile. If a resolution of say 0.5 pm in the Doppler profile is required the permissible variation in B is only a few percent.

Scheme (b) for Mo I has the major advantage that the strongest component of the π polarized absorption (see Fig. 9) is not Zeeman shifted, so if the laser wavelength is scanned through this component the resulting Doppler profile should be unaffected by variations in B. Because there is no π polarized M=0 to 0 fluorescence (see Fig. 10), it is necessary to observe the fluorescence in σ polarized emission. A FWHM detector filter bandwidth of 2.3 nm should be adequate up to B=10 T.

Scheme (b) is thus preferable to Scheme (a) for Doppler measurements on FTU, provided that the magnetic field is sufficiently strong for the separation between adjacent Zeeman components in the absorption line at 346.7 nm to be greater than the total breadth of the Doppler profile of interest. Scheme (a) might be preferable at very high temperatures or using low magnetic fields.

When a sufficiently narrow band laser with π or σ polarization is used to excite a line with a non-degenerate Zeeman pattern in a magnetic field, only one of the Zeeman components of the upper level can be excited at a time. This may considerably reduce the fluorescence signal as compared to the case of a line with a degenerate Zeeman pattern. Also, it should be noted that when only one of the magnetic states is excited, the spontaneous lifetime of the excited state will depend on the sum of the rates of all allowed transitions *from that state*, which may be significantly different from the normal averaged lifetime of the upper level, and should be

calculated. We have avoided this problem and assumed that each state of level 2 has the same lifetime, τ_2.

To estimate the performance of LIFS as applied to FTU we assume that sufficient laser power is available to approach saturation without causing unacceptable power broadening of the absorption transition. Adequate laser power should be available from the existing excimer-laser pumped dye laser at ENEA. The diagnostic optics on FTU are assumed to be as given by Borra [1993]. The fluorescence is detected by a photomultiplier with 2% quantum efficiency. Then we find that the number of photoelectrons collected, N_p, will be

for Fe, $N_p = 5.7 \times 10^{-15} n_0$

for Mo, $N_p = 1.8 \times 10^{-15} n_0$.

Measurements by McNeill et al. indicate that we can expect the plasma noise for the conditions assumed here, using a 10 nm filter bandwidth, to produce N_B=49 photoelectrons during an integration time of 100 ns at 380 nm (Fe I), while near 540 nm (Mo I) N_B=35. Signal-to-noise calculations then indicate that densities of about 1.5×10^{15} m^{-3} (Fe I) or 4.5×10^{15} m^{-3} (Mo I) should be detectable with a single laser pulse and a 2 nm filter bandwidth. If Doppler profiles are to be determined the densities must be three times larger, even if averages are taken over 10 laser pulses per point and the laser beam diameter is twice that assumed by Borra. These figures can, however, be much improved if larger optics be installed on FTU.

INDEX

LASER INDUCED FLUORESCENCE SPECTROSCOPY FOR FTU

1 - INTRODUCTION

Laser induced florescence spectroscopy (LIFS) is based on the selective, resonant absorption of tuned, pulsed laser light by a group of atoms of a particular species and the observation of the resulting fluorescence radiation from the excited state. Because the excitation is resonant it is very efficient, and the fluorescence can be many times brighter than the normal spontaneous emission, so low number densities of the selected atoms can be detected and measured. Good spatial resolution can be achieved by observing the emission from atoms in a short length of a narrow laser beam. If the laser is sufficiently monochromatic, and it can be tuned during a sequence of pulses over the absorption line profile of the selected atoms, information can be obtained about the Doppler and Zeeman effects which contribute to the line broadening and shift. Thus in principle LIFS can provide information about the density and the velocity of selected atoms, and also about the local magnetic field. The subject has recently been reviewed [1].

In most applications of LIFS in plasma diagnostics the laser light must pass through a window. The material that transmits the shortest wavelengths is lithium fluoride, and this sets a lower limit to the laser wavelength of about 120 nm. The largest possible single photon excitation energy is therefore about 10 eV. The technique is thus more useful for neutral atoms than for ions. It is most effective when the atoms are in the ground state, which is normally the most highly populated.

LIFS has been shown to provide valuable diagnostic information about impurity atom densities and fluxes in the cool edge region of tokamaks and other plasma machines. For example, the technique has enabled measurements to be made of the density of neutral iron atoms near a stainless steel limiter in the small ISX-B tokamak at Oak Ridge National Laboratory (ORNL) with a detection limit of 10^{12} to 10^{13} m^{-3} [2]. Measurements of neutral iron atoms were also made near the wall of the Heliotron E device [3]. On Textor at Julich Fe I density measurements of about 4×10^{15} m^{-3} were made which, when combined with estimates of velocities, gave neutral iron atom flux measurements of order 10^{19} m^{-2} s^{-1} [4]. On the Elmo Bumpy Torus at ORNL neutral aluminium atom densities of order 10^{13} m^{-3} were recorded near the walls and velocities of order 2 km s^{-1} were measured, giving the flux of aluminium atoms, of order 10^{17} m^{-2} s^{-1} [5]. The spatial distribution of beryllium densities, of order 10^{15} m^{-3} was measured near a beryllium poloidal limiter in the Unitor tokamak at Düsseldorf [6].

At ENEA, extensive preparatory work, both theoretical and experimental, has been done by G. Gatti with the intention of using LIFS as an edge plasma diagnostic on the FTU tokamak.

The objective is to make measurements of densities and, if possible, of velocities, and hence of fluxes, of neutral iron and molybdenum atoms emitted from plasma limiters in FTU. On the basis of emission spectroscopic observations the Fe I density in the edge plasma near a limiter has been estimated to be about 4×10^{15} m^{-3} [7,8]. Near the molybdenum limiter the Mo I density may be somewhat lower because of the larger limiter area. As a preliminary test a tunable, excimer-laser-pumped dye laser at ENEA has been successfully used to determine the density of neutral iron atoms near a stainless steel electrode bombarded by argon ions in a 1.1 keV discharge [9]. Calculations by Borra [9], based on this work and on the emission spectroscopy on FTU, predict that it will be possible to obtain satisfactory measurements of iron atom densities in the edge region of FTU using LIFS.

The present report considers the application of LIFS to studies of density and velocity measurements of both iron and molybdenum atoms in the edge plasma of FTU. Two topics of particular importance are examined in detail. The first is the effect of high laser irradiance on the apparent absorption line profile, which is often known as "power broadening" or "saturation broadening". The second is the effect of the high magnetic field in FTU on the LIFS transitions. We begin by outlining the general theory of LIFS in Sec. 2, which leads to a discussion of power broadening. The effects of a magnetic field are described in Sec. 3. In Secs. 4 and 5 detailed calculations are given for LIFS of neutral iron and molybdenum atoms, including the Zeeman effect. The implementation of LIFS for these atoms on FTU is discussed in Sec. 6. The conclusions are summarised in Sec. 7.

2 - THEORY OF LASER INDUCED FLUORESCENCE SPECTROSCOPY

In this section we give the theory of LIFS, first for a two-level atom and then for what is generally known as a "three-level" atom.

2.1 - Two-level atom

Consider first an atom with only two levels. Figure 1 shows the three possible radiative transitions between the two levels. $B_{12}U$ is the absorption rate per atom, $B_{21}U$ is the stimulated emission rate and A_{21} the spontaneous emission rate. g_1, g_2 are the statistical weights, or degeneracies, of levels 1 and 2, whose populations are n_1, n_2 per unit volume. U is the spectral energy density of isotropic radiation at frequency ν, in J m^{-3} Hz^{-1}, assumed constant over the absorption line bandwidth.

The Einstein coefficients A_{21}, B_{21} and B_{12} are related by

$$g_1 B_{12} = g_2 B_{21},$$

$$\frac{A_{21}}{B_{21}} = \frac{8\pi h\nu^3}{c^3} \qquad (1)$$

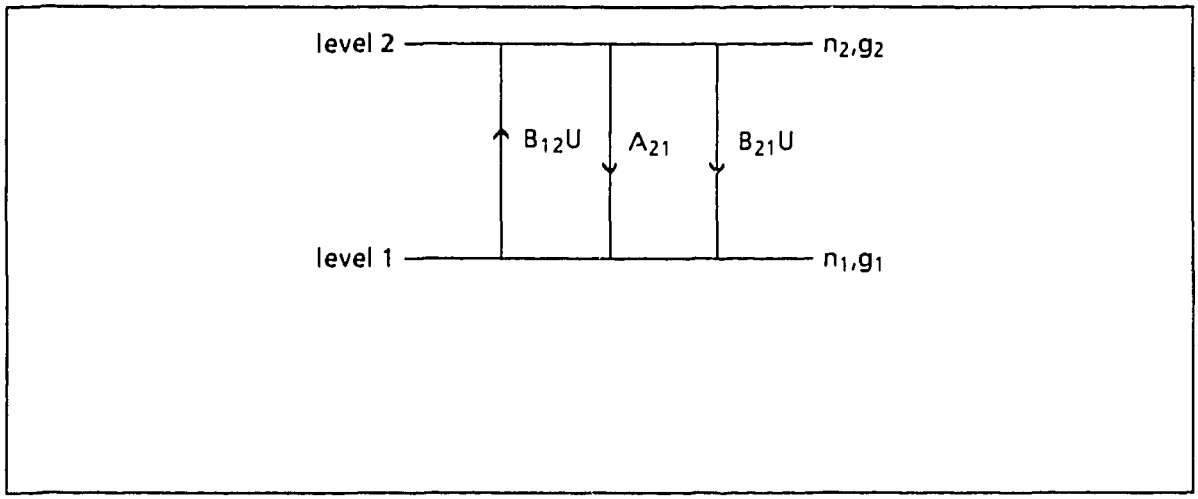

Fig. 1 - Two-level system

The rate equations are

$$\frac{dn_1}{dt} = -B_{12}Un_1 + (A_{21} + B_{21}U)$$

$$\frac{dn_2}{dt} = -\frac{dn_1}{dt} \tag{2}$$

Suppose initially n_2=0, n_1=n_{10}. Suppose also U is constant with time. Then when an equilibrium is reached so that $\frac{dn_1}{dt} = \frac{dn_2}{dt} = 0$,

$$\frac{n_2}{n_{10}} = \frac{g_2}{g_1 + g_2}\left[1 + \frac{g_1}{g_1 + g_2}\frac{A_{21}}{B_{21}U}\right]^{-1} \tag{3}$$

We can write the second term inside the bracket as $1/S_2$ (where the subscript 2 denotes a two-level atom), so

$$S_2 = \frac{g_1 + g_2}{g_1}\frac{B_{21}}{A_{21}}U = \frac{g_1 + g_2}{g_1}\frac{c^3}{8\pi h\nu^3}U. \tag{4}$$

Then (3) becomes

$$\frac{n_2}{n_{10}} = \frac{g_2}{g_1 + g_2}\frac{S_2}{1 + S_2} \tag{5}$$

S_2 is known as the *saturation parameter* for a two-level system.

At equilibrium, if also S_2 =0 then n_2=0 , while if

$$S_2 = 1, \qquad \frac{n_2}{n_{10}} = \frac{1}{2}\frac{g_2}{g_1 + g_2}, \tag{6}$$

and if

$$S_2 = \infty, \qquad \frac{n_2}{n_{10}} = \frac{g_2}{g_1 + g_2},$$

this last being the maximum possible value of n_2 / n_{10}. Thus in order to excite half the maximum possible fraction of the atoms to the upper level, we need S_2=1, i.e.

$$(S_2 = 1) \qquad U = \frac{8\pi h\nu^3}{c^3}\frac{g_1}{g_1 + g_2}.$$

In terms of spectral irradiance I_ν,

$$(S_2 = 1) \qquad I_\nu = \frac{8\pi h\nu^3}{c^2}\frac{g_1}{g_1 + g_2} \quad \mathrm{Wm^{-2}Hz^{-1}}.$$

2.2 - "Three-level" atoms

In the present context a "three-level" atom is defined as an atom with one or more additional levels, between levels 1 and 2, to which level 2 can decay, and which have a long radiative lifetime compared to the duration of the laser pulse in a fluorescence experiment (Fig. 2). Once an atom makes the transition into such a level it is assumed to take no further part in the interaction with the laser radiation. All the levels in this category can thus be lumped together in the rate equations. Suppose there are (m-2) such levels. The rate equations now become

$$\frac{dn_1}{dt} = -B_{12}Un_1 + (A_{21} + B_{21}U)n_2$$

$$\frac{dn_2}{dt} = -\frac{dn_1}{dt} - \sum_{k=3}^{m} A_{2k}n_2$$

$$\frac{dn_{3\bullet}}{dt} = \sum_{k=3}^{m} A_{2k}n_2, \tag{7}$$

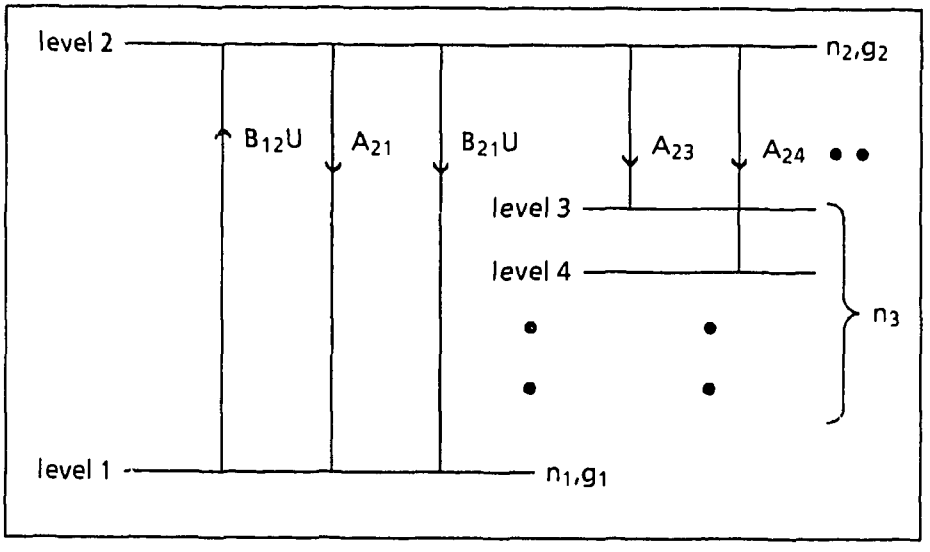

Fig. 2 - Three-level system

where $n_{3*} = \sum_{k=3}^{m} n_k$.

Equations (7) are quite general and apply for any time dependent laser pulse $U(t)$. Analytic solutions are only found for special cases.

In the case where U is constant throughout the laser pulse an analytic solution has been given by Dullni [5]. The saturation parameter for this system, S is defined by

$$S = \frac{g_1 + g_2}{g_1} \frac{B_{21}}{A_{21} + \sum_{k=3}^{m} A_{2k}} U. \tag{8}$$

We denote the spontaneous lifetime of level 2 by

$$\tau = \frac{1}{A_{21} + \sum_{k=3}^{m} A_{2k}}. \tag{9}$$

Then

$$S = \frac{g_1 + g_2}{g_1} A_{21} \tau \frac{c^3}{8\pi h \nu^3}. \tag{10}$$

For a laser beam with a spectral bandwidth $\Delta\nu_L$ which is substantially wider than the atomic line width we may write

$$U = \frac{I_L}{c\Delta\nu_L} = \frac{I_\nu}{c}, \tag{11}$$

where I_L is the laser irradiance (power per unit area of the beam) and I_ν is the spectral irradiance (power per unit area per unit frequency). Then in convenient units

$$S = 6.67 \frac{g_1 + g_2}{g_1} A_{21} \tau \frac{\lambda^5(\text{mm})}{\Delta\lambda_L(\text{pm})} I_L, \tag{12}$$

with I_L in W cm^{-2}.

Under these conditions the solution to the rate equations (7) for constant laser irradiance, assuming that initially $n_1 = n_{10}$, $n_2 = n_{3*} = 0$, is given by Dullni [5] as

$$\frac{n_2(t)}{n_{10}} = \frac{g_2}{g_1 + g_2} \frac{S}{R} \exp\left(-\frac{t}{2\tau}[1 + S - R]\right) \cdot \left\{1 - \exp\left(-\frac{Rt}{\tau}\right)\right\}, \tag{13}$$

where

$$R = \left[(1+S)^2 - 4S\frac{g_2}{g_1 + g_2}(1 - A_{21}\tau)\right]^{1/2}. \tag{14}$$

Sample values of S and R are given in Table I.

It is important to note that the solution to the rate equations given in (13) applies only for constant laser irradiance. For a real laser pulse the equations (7) must be solved with a time dependent U: S is then also a function of time. In contrast to the two-level system, there is no steady state until, after a long time, n_2 falls to zero.

TABLE I

Atomic parameters for possible LIFS experiments

Fe I:	a^5D_4 (1)	→ (302.06 nm)	$y^5D_4°$ (2)	→ (382.04 nm)	a^5F_5 (3)
Mo I: Scheme (a)	a^7S_3 (1)	→ (345.6 nm)	$z^5P_3°$ (2a)	→ (550.6 nm)	a^5S_2 (3)
Mo I: Scheme (b)	a^7S_3 (1)	→ (346.7 nm)	$z^5P_2°$ (2b)	→ (553.3 nm)	a^5S_2 (3)

	Fe I	**Mo I** Scheme (a)	**Mo I** Scheme (b)
g_1	9	7	7
g_2	9	7	5
A_{21}	$75.9\times10^6 s^{-1}$	$2.1\times10^6 s^{-1}$	$1.29\times10^6 s^{-1}$
A_{23}	$72.9\times10^6 s^{-1}$	$36.1\times10^6 s^{-1}$	$37.2\times10^6 s^{-1}$
$\sum_{k=3}^{m} A_{2k}$	$94.6\times10^6 s^{-1}$	$47.6\times10^6 s^{-1}$	$49.2\times10^6 s^{-1}$
τ_2	5.9 ns	20.1 ns	19.8 ns

Sample values of R and S (see Eqs. (12) and (14))

For $I_L = 1.6\times10^8$ W m^{-2} and $\Delta\lambda_L = 5$ pm,

	Fe I	**Mo I** Scheme (a)	**Mo I** Scheme (b)
S	48	8.88	4.7
R	48.5	8.98	4.99
S/R	0.99	0.99	0.94
$1+S-R$	0.5	0.9	0.71

Suppose then that we have a solution for the rate equations of the form

$$n_2 = n_2(t). \tag{15}$$

It can be useful to define a parameter

$$\eta = \frac{1}{n_{10}} \int_0^\infty n_2(t)dt \cdot \sum_{k=3}^{m} A_{2k} \tag{16}$$

- the "pumpover efficiency". This is the fraction of all the atoms originally in the ground state (n_{10} per unit volume) that go over into any of the levels k ($3 \le k \le m$) during the laser pulse. Two limiting cases are of interest.

(i) For a long, high power pulse $\eta \to 1$.

(ii) for a very high power pulse whose duration t_L is very short compared to the decay time of level 2, the maximum possible number of atoms will be pumped into level 2 during the pulse, so

$$n_2(t_L) = n_{10} \frac{g_2}{g_1 + g_2}$$

(which is the same as the two-level result for $S_2=\infty$), and after the pulse has ended the atoms decay spontaneously, so

$$\eta \approx \frac{g_2}{g_1 + g_2} \sum_{k=3}^{m} A_{2k} \tau. \tag{17}$$

Experimentally, what is measured is the number of fluorescence photons produced in the $2 \to 3$ transition. In all cases this is given, per unit volume, by

$$n_F = \int_0^\infty n_2 dt \cdot A_{23} \tag{18}$$

or

$$n_F = \frac{A_{23}}{\sum_{k=3}^{m} A_{2k}} \cdot n_{10} \eta. \tag{19}$$

Since the maximum possible value of η is 1, the maximum possible number of fluorescence photons that can be produced per unit volume by a long, high power laser pulse is

$$n_{F_{\max}} = \frac{A_{23}}{\sum_{k=3}^{m} A_{2k}} \cdot n_{10} \tag{20}$$

For the short, high power pulse

$$n_F \approx A_{23}\tau \frac{g_2}{g_1 + g_2} \cdot n_{10} \tag{21}$$

Table I shows atomic parameters for transitions of interest in Fe I and Mo I which will be considered in detail in Secs. 4 and 5 below. Using these values we find

	Fe I (382.0 nm)	**Mo I** (550.6 nm)	**Mo I** (553.3 nm)
$\frac{n_{F_{\max}}}{n_{10}} =$	0.77	0.76	0.76
$\frac{n_{F_{\text{short pulse}}}}{n_{10}} =$	0.22	0.36	0.31

Thus for one of these transitions a very intense short laser pulse should cause up to about one fifth of the Fe atoms, or one third of the Mo atoms, to fluoresce, and a long high power pulse could increase the proportions to three quarters.

For intermediate pulse lengths and intensities we can make use of Dullni's [5] result (expression (13) above) for $n_2(t)$. Assuming a constant laser irradiance, with a pulse duration t_L, the total number of fluorescence photons emitted per unit volume, i.e. the sum of those emitted during the pulse and those emitted after it ends, will be

$$n_F = A_{23} \int_0^{t_L} n_2(t)dt + A_{23}\tau n_2(t_L).$$

From (13) and (14),

$$\frac{n_F}{n_{10}} = \frac{g_2}{g_1+g_2}\frac{S}{R}\left[\frac{1-\exp\left(-F\frac{t_L}{\tau}\right)}{F} - \frac{1-\exp\left(-[F+R]\frac{t_L}{\tau}\right)}{F+R}\right.$$

$$\left. + A_{23}\tau\exp\left(-F\frac{t_L}{\tau}\right)\left(1-\exp\left[-R\frac{t_L}{\tau}\right]\right)\right], \qquad (22)$$

where $F = (1-S-R)/2$.

Figure 3 shows n_F/n_{10} as a function of S for the Fe absorption line at 382.0 nm, for four different values of t_L/τ. For a very short pulse $(t_L/\tau = 0.1)$ nearly all the fluorescence occurs after the pulse ends: the total emission approaches the short pulse limit of $n_F/n_{10} = 0.22$ for large S, and reaches half this value at $S \approx 7$. When $t_L/\tau = 0.5$, the limit increases to $n_F/n_{10} \approx 0.29$ and half this limit is reached with $S \approx 2$. When $t_L/\tau = 2$, this limit is $n_F/n_{10} \approx 0.45$, and $n_F/n_{10} = 0.22$ is reached with $S \approx 5$: with this relatively long pulse, most of the emission occurs during the pulse. Finally, when $t_L/\tau = 20$, the long pulse limit of $n_F/n_{10} \approx 0.77$ is approached for $S \approx 2$.

For a real laser pulse it is necessary to integrate the rate equations (7) numerically to determine $n_2(t)$. Results have been published for a Gaussian pulse shape [9] and for a sine function [5]. Having found $n_2(t)$ we must integrate again to obtain the fluorescence output n_F.

2.3 *The absorption line profile*

Until now, we have supposed that the laser radiation is spectrally flat, with a spectrum sufficiently broad to cover the entire bandwidth of the absorption line of interest for all the atoms in the interaction volume, including any Doppler shifts due to movement with velocity components along the beam. On this assumption all atoms have equal chances of being pumped from level 1 to level 2. In LIF measurements an interference filter is placed in front of the detector to isolate the fluorescence line of interest, but we collect all the fluorescence photons emitted within a selected solid angle without any attempt at detailed spectral analysis. Such a system, with a broad band laser source, can tell us nothing about the spectral profiles of the absorption or the fluorescence lines, and thus nothing about the velocity distribution of the atoms. In order to obtain velocity information from LIFS measurements we must spectrally resolve the Doppler profile of either the absorption line or the fluorescence line. Because the fluorescence signal is weak it is preferable to use a relatively narrow bandwidth laser, and scan its central wavelength over the absorption line profile, while collecting the fluorescence photons without spectral analysis. We must now modify our calculations appropriately. We

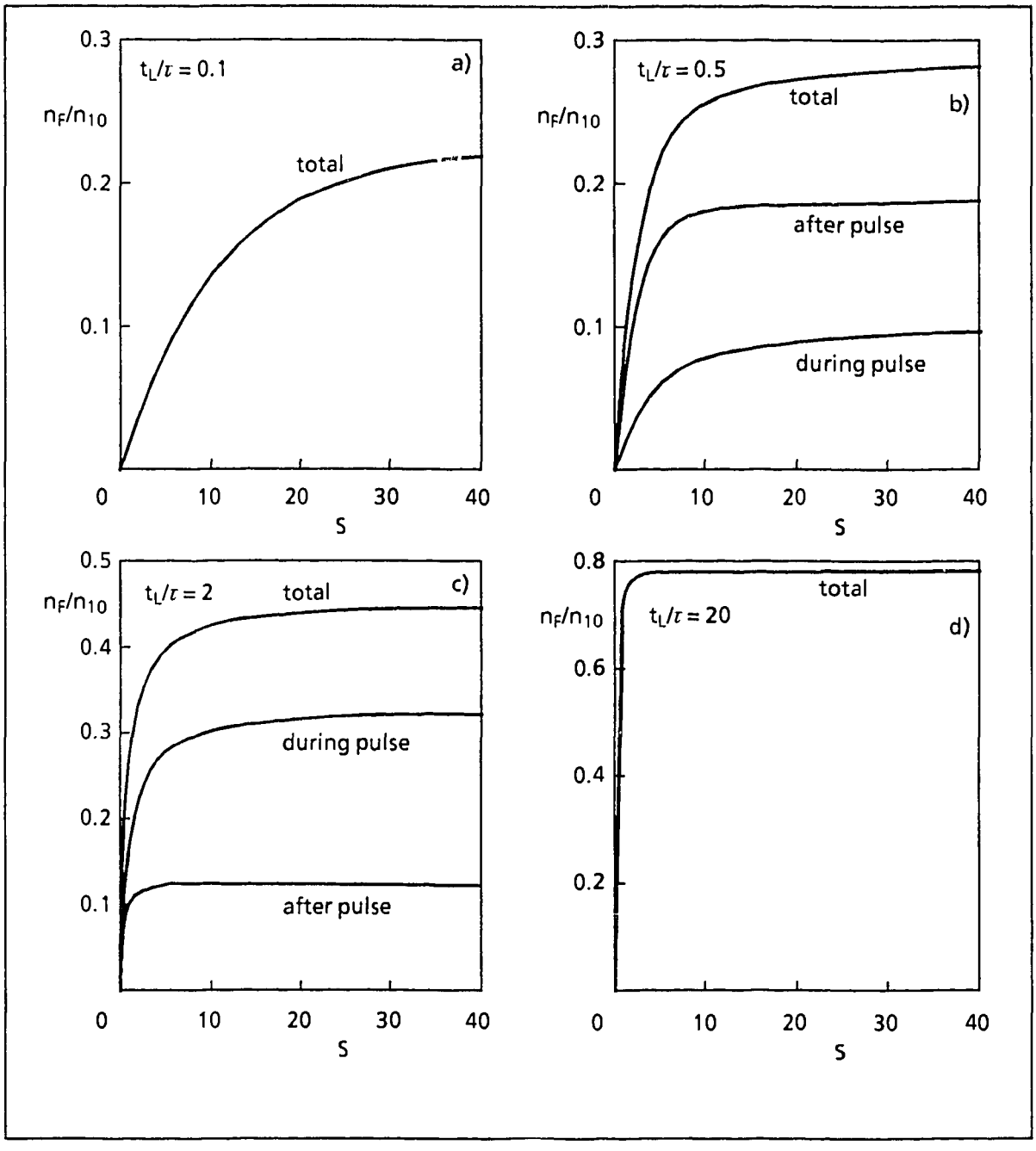

Fig.3 - Fluorescence photon yield from Fe I as a function of S for four laser pulse durations

begin by considering the relationships between the radiation energy density and the transition rates in greater detail, following a treatment given in Ref. [10].

2.3.1 Energy density and transition rates

So far we have taken the usual expressions for the transition rates per atom, e.g.

$$W_{12} = B_{12}U. \tag{23}$$

No mention was made of the absorption line profile, because it was assumed that U, or more precisely $U(\nu)$, the energy density per unit frequency bandwidth at ν, was constant over the frequency region of the absorption line.

If, instead, we had had monochromatic radiation, with energy density U_ν at ν (*not* per unit frequency bandwidth), then we would have had to include the line shape function of the atomic absorption transition, denoted by $g(\nu)$, with dimension Hz^{-1}, which is normalised so that

$$\int_{-\infty}^{\infty} g(\nu)d\nu = 1$$

Then

$$W_{12} = B_{12} \cdot U_\nu \cdot g(\nu). \tag{24}$$

From (1), we may therefore write for monochromatic radiation at ν,

$$W_{12} = A_{12}\frac{c^3}{8\pi h\nu^3} \cdot U_\nu \cdot g(\nu). \tag{25}$$

If the laser radiation is neither very broad nor monochromatic, but has energy density per unit frequency bandwidth $U(\nu)$ which varies significantly over the bandwidth of the absorption line, we must incorporate both $U(\nu)$ and the absorption lineshape function. In this general case,

$$W_{12} = A_{12}\frac{c^3}{8\pi h}\int_{-\infty}^{\infty} \frac{U(\nu)\cdot g(\nu)}{\nu^3}d\nu. \tag{26}$$

This expression still works for very broad band radiation: in this case, if the absorption line profile is only appreciable in a narrow frequency band around ν, the value of $U(\nu)$ is essentially constant where $g(\nu)$ is not negligible, so we may take $U(\nu)$, and also ν^3 for a narrow absorption line, outside the integral. Then

$$W_{12} = A_{12}\frac{c^3}{8\pi h\nu^3}U(\nu)\int_{-\infty}^{\infty} g(\nu)d\nu \tag{27}$$

so, from the normalisation condition for g, in this case

$$W_{12} = B_{12}U(\nu)$$

as in (23).

Expression (26) is still valid when the two profile are centred at different frequencies. If the central frequency of the laser profile ν_L, is initially set at a frequency away from the absorption line centre and is then swept through it, the transition rate will vary with ν_L in a way which depends on both profiles. In the case when both the profiles are Lorentzian, the breadth of the resulting absorption profile, as a function of the laser central frequency, will be the square root of the sum of the squares of the two half widths (a different result is obtained if one of the profiles is a Gaussian).

W_{12} and W_{21} determine the response of the atoms to the laser beam. If the atomic line profile is due only to natural broadening, all atoms will have the same absorption profile, and the resultant broadening of W_{12} will be the same for all atoms; the broadening is *homogeneous*.

If we are to use this method to determine the absorption line profile, for example to find the velocity distribution from the Doppler effect, we must have a laser frequency profile which is narrow compared to the line profile. Doppler broadening is usually much larger than the natural line width (see Table II). Within the population of atoms illuminated by a narrow band laser, only that group of atoms whose Doppler shifted natural line profile overlaps the laser profile will absorb. Doppler broadening is thus *inhomogeneous*, and the response of each group of atoms must be calculated and summed.

2.3.2 Power broadening

This is also known as saturation broadening. It arises because the fluorescence intensity is not a linear function of the laser output power, but approaches a maximum (i.e. saturates) as the power is increased.

Let us consider a hypothetical LIFS experiment in which a laser with a certain spectral profile is scanned in frequency over an almost monochromatic atomic line. The *apparent* width of the laser profile, as determined from the absorption and the resulting fluorescence output during the frequency scan, will depend on the laser power, and will be broader for higher laser powers. This is because in the centre of the profile the absorption (and hence the fluorescence signal) is nearest to its saturation value. With increasing laser power, the absorption (and hence the fluorescence) can increase in the wings of the laser profile more than in the centre. This results in an increase in the apparent halfwidth of the laser profile.

An exactly similar effect would be seen if a monochromatic laser was scanned over a homogeneously broadened line profile. If both the laser and the atomic line profiles have finite widths, the resulting overall homogeneous profile will be broadened by saturation which will depend on both profiles.

TABLE II

Some relevant frequencies

Natural breadths of atomic upper levels for the proposed LIFS transitions		
Fe I:	$\Delta\nu_N = 1/2\pi\tau$ =27 MHz	$\Delta\lambda$ (absorption line)=0.008 pm
Mo I Scheme (a):	7.9 MHz	0.0031 pm
Mo I Scheme (b):	8.0 MHz	0.0032 pm
Assumed breadth of a single laser mode		~100 MHz
Typical dye laser mode spacing (350 mm cavity length)		~430 MHz
Doppler shift corresponding to v=2 km s^{-1}		= 6.6 GHz (Fe) 5.8 GHz (Mo)
Typical dye laser bandwidths		
(with etalon)$\Delta\lambda_L$~ 1 pm $\rightarrow \Delta\lambda_L$		~3 GHz for λ = 302 n 2.5 GHz for λ = 346 nm (Mo I)
or (no etalon)	5 pm	~16 GHz (Fe I) 13 GHz (Mo I)

The effect is easy to calculate for a 2 level atom. We assume first that the laser energy density U has a Lorenztian frequency profile, centred at a frequency ν_L which is varied during the scan. From Eq. (4) the 2 level saturation parameter S_2 will also have a Lorenztian profile, with maximum value S_0=$S_2(\nu_L)$ and full width at half maximum (FWHM) of $\Delta\nu_L$, assuming the atomic line is narrow:

$$S_2(\nu-\nu_L)=\frac{(\Delta\nu_L/2)^2}{(\nu-\nu_L)^2+(\Delta\nu_L/2)^2}\cdot S_0. \tag{28}$$

If we put this expression for S_2 into Eq. (5) for the population density of the upper level, n_2, we find

$$\frac{n_2}{n_{10}} = \frac{g_2}{g_1 + g_2} \frac{(\Delta\nu_L/2)^2}{(\nu - \nu_L)^2 (\Delta\nu_L/2)^2 (1 + S_0)} \cdot S_0 \tag{29}$$

which is a new Lorentzian with increased halfwidth

$$\Delta\nu_L = \Delta\nu_L \sqrt{1 + S_0}. \tag{30}$$

(Lorentzian)

This is the standard result. If the atomic resonance has a homogeneous breadth of $\Delta\nu_{12}$, then

$$\Delta\nu = \left(\Delta\nu_L^2 + \Delta\nu_{12}^2\right)^{1/2} \sqrt{1 + S_0}. \tag{31}$$

(homogeneous)

Dullni [5] also considered the case of a narrow atomic resonance and a Gaussian laser frequency profile, and found that in this case

$$S_2(\nu - \nu_L) = \exp\left[-\left(\frac{\nu - \nu_L}{\Delta\nu_L/2}\right)^2 \ln 2\right]. \tag{32}$$

The resulting power broadened FWHM is

$$\Delta\nu_L = \Delta\nu_L \sqrt{\frac{\ln(2 + S_0)}{\ln 2}} \tag{33}$$

(Gaussian)

which is smaller than that for the Lorenztian profile (30).

The two-level theory of power broadening was carefully tested experimentally tested (see Ref.[11]) using specially pumped Na I atoms in an atomic beam. In these experiments the laser width was small, and the apparent broadening of the atomic transition was measured. It was closely Lorentzian and agreed very accurately with theory.

In the case of a three-level atom the effect is not so easily calculated. Dullni described an experiment in which a laser was scanned in frequency over a narrow resonance line of Ti I in a collimated vapour beam. The scan was repeated at a different laser output. The fluorescence intensity measured at each wavelength setting during the scan gave the power broadened apparent profile of the laser line. The observations were close to those expected on the basis of two-level theory for a Gaussian profile, and much narrower than was expected for a Lorentzian. It should be noted, however, that the two-level theory is not valid for this experiment, and a full calculation might modify the conclusions.

The mode structure of the laser radiation further complicates the theory. Table II gives examples of the spacing and breadth of the modes of a typical dye laser cavity. The spacing between the modes is often greater than the homogeneous width of the LIFS absorption line, which at low plasma densities is not much greater than the natural linewidth, so each mode will tend to interact with only a small fraction of the population of absorbing atoms. For those interacting atoms, however, the effective value of the saturation parameter will be correspondingly greater than the average over the full laser bandwidth. This aspect of power broadening deserves further careful study.

Preliminary measurement of power broadening in LIFS experiments at ENEA, using sputtered Fe I atoms, have been reported [9]. Using a 10 ns laser pulse with an estimated bandwidth of 5 pm, and scanning the laser wavelength through the 302 nm region, little or no power broadening was found in the 302.06 nm Fe I absorption line at a laser irradiance of about 2×10^6W m^{-2} (i.e. a spectral irradiance of about 4×10^5W m^{-2} pm^{-1}.) However, when the laser irradiance was increased to about 2×10^7W m^{-2}, the absorption line appeared to be strongly broadened to a FWHM of about 12 pm. This is consistent with a comment by Bogen and Hintz [12] that the irradiance should be less than about 5×10^6W m^{-2} if power broadening is to be avoided for this line, although the laser bandwidth which they were considering was not specified. The measurements on Fe I at ENEA will be extended, andmeasurements with Mo I will also be possible.

From the point of view of LIFS experiments designed to study Doppler-modified absorption line profiles, the important consideration is to ensure that power broadening does not distort the profile. All that is necessary is to determine the maximum allowable laser power per unit area in a given situation. Experimental tests with different laser powers will readily show whether power broadening is a problem, and may enable a correction to be made, as was necessary, for example, in the work described in Refs. [13,14].

2.4 - Anisotropy and polarization

The theory given above assumes that the laser radiation is isotropic and neglects polarization effects. In practice a narrow, collimated laser beam is used, and (as will be seen from the following sections) when a magnetic field is present polarization effects are important. In the present paper we shall assume that the laser beam is linearly polarized and propagates perpendicularly to the magnetic field.

3 - EFFECT OF A MAGNETIC FIELD

3.1 - Zeeman splitting of energy levels

The strong magnetic field of order 10 Tesla in FTU can cause significant Zeeman splitting of the atomic energy levels into separate magnetic states. For an atom with LS coupling in weak

fields, the change in energy of an atomic state with magnetic quantum number M in a magnetic field B Tesla, from the unperturbed energy, is given by

$$\Delta W = 9.27 \times 10^{-24} \mathrm{M} g_L B \quad \mathrm{J} \tag{34}$$

where g_L is the Landé factor for the level, which is given approximately by

$$g_L = 1 + \frac{\mathrm{J(J+1)} + \mathrm{S(S+1)} - \mathrm{L(L+1)}}{2\mathrm{J(J+1)}} \tag{35}$$

Experimental values are often available (see, e.g. Ref. [15]). The weak field theory breaks down when the Zeeman shift is comparable to or greater than the fine structure splitting.

Transitions between the magnetic states of two levels are only allowed if ΔM, the change in M, is equal to ±1 or 0. The polarization of the radiation emitted depends on which of these conditions is obeyed: for emission perpendicular to the magnetic field, if ΔM=0 the emission is "π" polarized, with the electric field parallel to B. If ΔM=±1, the emission is "σ" polarized, with the electric field perpendicular to B.

The emission spectrum due to transitions between two energy levels will consist of the contributions from all the allowed transitions between the magnetic states. If the upper and lower states have different Landé factors, the emission spectrum will consist of components from all the allowed transitions, with wavelength shifts given by

$$\Delta\lambda = 4.67 \times 10^{-5} \lambda^2 (\mathrm{M}_1 g_{L1} - \mathrm{M}_2 g_{L2}) B \quad \mathrm{pm} \tag{36}$$

where λ is in nm and B in Tesla.

If the upper and lower states have the same Landé factors, the emission spectrum will consist of only three lines (this degenerate case was originally described as the "normal" Zeeman effect). The π component, which contains all the ΔM=0 transitions, will be unshifted. The two σ components, one containing all the ΔM=+1 and the other all the -1 transitions, will be shifted equally to higher and lower frequencies: in terms of wavelength, for a line at wavelength λ, they are displaced by

$$\Delta\lambda = \pm 4.67 \times 10^{-5} \lambda^2 g_L B \quad \mathrm{pm}. \tag{37}$$

3.2 - Intensities of Zeeman components

The relative intensities of the Zeeman components of a line may be calculated from the following formulae given e.g. in Ref. [16], which assume equal populations of the 2J+1 magnetic states of the excited level. For transitions between a state with total angular

momentum quantum number J and magnetic quantum number M ($-J \leq M \leq J$), and a state with J' and M':

If $J'=J$, then

for $M'=M+1$, $I=(A/2)(J-M)(J+M+1)$

for $M'=M$, $I=AM^2$

for $M'=M-1$, $I=(A/2)(J+M)(J-M+1)$ (38)

or if $J'=J+1$, then

for $M'=M+1$, $I+(B/2)(J+M+1)(J+M-2)$

for $M'=M$, $I=B(J+1)^2-M^2$

for $M'=M-1$, $I=(B/2)(J-M+1)(J-M+2)$ (39)

or if $J'=J-1$, then

for $M'=M+1$, $I=(C/2)(J-M)(J-M-1)$

for $M'=M$, $I=C(J^2-M^2)$

for $M'=M-1$, $I=(C/2)(J+M)(J+M-1)$. (40)

The constants A, B and C depend on the states involved. The sum of the Zeeman component intensities (which are integrated over all directions) is equal to the transition probability A_{21} between the energy levels. However, the emission is not isotropic: the relative intensities emitted in a particular direction depend on the angle between this direction and the direction of the magnetic field. For $\Delta M=M-M'=\pm 1$, i.e. for σ components,

$$I(\theta) = I\left(1+\cos^2\theta\right)/2, \tag{41}$$

while for $\Delta M=0$ (π components)

$$I(\theta) = I\sin^2\theta. \tag{42}$$

Thus when emission is observed at 90° to the magnetic field the relative intensities of the σ components calculated from the expressions above, and plotted in the usual Zeeman patterns, must be divided by two.

3.3 - Effect of excitation by a polarized beam

If atoms are excited to an upper state in an electric dipole transition due to a linearly polarized beam of radiation, they will be polarized. As a result, dipole emission due to subsequent transitions from the excited state will tend to be polarized also. However, in even a small magnetic field (~10^{-4}T) resonance radiation is depolarized: this is known as the Hanle effect and is due to precession of the emitting dipole round the magnetic field direction. At high fields of order 1 T the precession is so rapid (many GHz) that only the usual Zeeman pattern will be observed. Thus in the conditions envisaged in FTU the direction of polarization of the linearly polarized laser beam will have no perceptible effect on the Zeeman pattern of the fluorescence radiation, which will be determined only by the direction of observation, relative to that of the magnetic field.

4 - LIFS CALCULATIONS FOR Fe I ATOMS

4.1 - Selection of LIFS transitions

Accurate values of level energies and lifetimes and transition probabilities between levels are available for Fe I [17]. The ground term of Fe I is a^5D, and absorption to y^5D^0, is suitable for LIFS with laser wavelengths near 300 nm. If the populations of the levels of the ground term with J=0,1,2,3,4 are n_J, their ratios may be estimated from the Boltzmann relationship, using known energy level spacings and degeneracies g_J, if we assume an excitation temperature T:

$$\frac{n_a}{n_b} = \frac{g_a}{g_b} \exp\left(\frac{E_a - E_b}{k_B T}\right). \tag{43}$$

Thus at T=0 all the atoms will be in the lowest level, while at T=∞

$$\frac{n_3}{n_4} = \frac{7}{9}, \quad \frac{n_2}{n_4} = \frac{5}{9}, \quad \frac{n_1}{n_4} = \frac{3}{9}, \quad \frac{n_0}{n_4} = \frac{1}{9},$$

so the lowest possible thermal equilibrium value of n_4 is 9/25 or 36% of the total number of atoms in the ground term. The populations of the levels in sputtered iron atoms have been investigated and found to correspond to an excitation temperature near 1000 K [18, 19]. Taking T=1000 K,

$$g_J = 2_J + 1, \quad E_4 = 0, \quad E_3 = 416\ \text{cm}^{-1},$$
$$E_2 = 704\ \text{cm}^{-1}, \quad E_1 = 888\ \text{cm}^{-1}, \quad E_0 = 978\ \text{cm}^{-1},$$

we find

$$\frac{n_3}{n_4} = 0.43, \quad \frac{n_2}{n_4} = 0.20, \quad \frac{n_1}{n_4} = 0.09, \quad \frac{n_0}{n_4} = 0.03,$$

so about 57% of the atoms will be in the lowest (J=4) level. We shall assume this value for the ratio: clearly it is not very sensitive to T in this region of temperature.

The spontaneous transition probabilities A_{21} for the stronger lines in the absorption multiplet are known [17] and can be used to find the absorption coefficients, because

$$B_{12} = \frac{g_2}{g_1} A_{21} \frac{c^3}{8\pi h \nu^3}. \tag{44}$$

It then becomes clear that the strongest absorption line, and the most suitable for LIFS excitation, is $a^5D_4 - y^5D_4^0$ at 302.064 nm. The two nearest of the other lines in this multiplet are $a^5D_2 - y^5D_2^0$ at 302.049 nm and $a^5D_3 - y^5D_3^0$ at 302.107 nm. These will be much weaker (less than about 5% of the strongest line), and are sufficiently well separated from the strongest line (by 15 and 43 pm respectively) to be normally well resolved, but their Zeeman splitting can be significant and will be considered in Sec. 4.2 below.

The fluorescence can conveniently be observed in the decay from y^5D^0 to a^5F. Assuming that the J=4 level is pumped by the laser, the strongest line in this multiplet will be $y^5D_4^0$ to a^5F_5 at 382.0425 nm [17]. Competing lines, the (4-4) and (4-3) transitions are not given in the list of strong lines, and are in any case separated from (4-5) by more than 6 nm, so they will not normally be detected.

We shall thus assume that Fe I atoms will be pumped near 302.06 nm from level 1, a^5D_4, to level 2, $y^5D_4^0$, and that fluorescence due to decay from level 2 to level 3, a^5F_5, will be measured near 382.04 nm.

4.2 - The Zeeman effect in Fe I

For both levels 1 and 2 of the Fe I LIFS scheme discussed above, J=4, L=2 and S=2, so from expression (35) g_L=1.5. The experimental value from Moore [15] is 1.496 in each case.

For level 3, J=5, L=3 and S=2, so from expressions (35) g_L=1.4, while the experimental value is 1.404.

Thus for the absorption line at 302.06 nm between levels 1 and 2 the Zeeman pattern is degenerate (Fig. 4). There is a single unshifted π polarized component consisting of the sum of all Δm=0 transitions. There are two σ components, shifted by ±6.35 B (Tesla) pm. It is

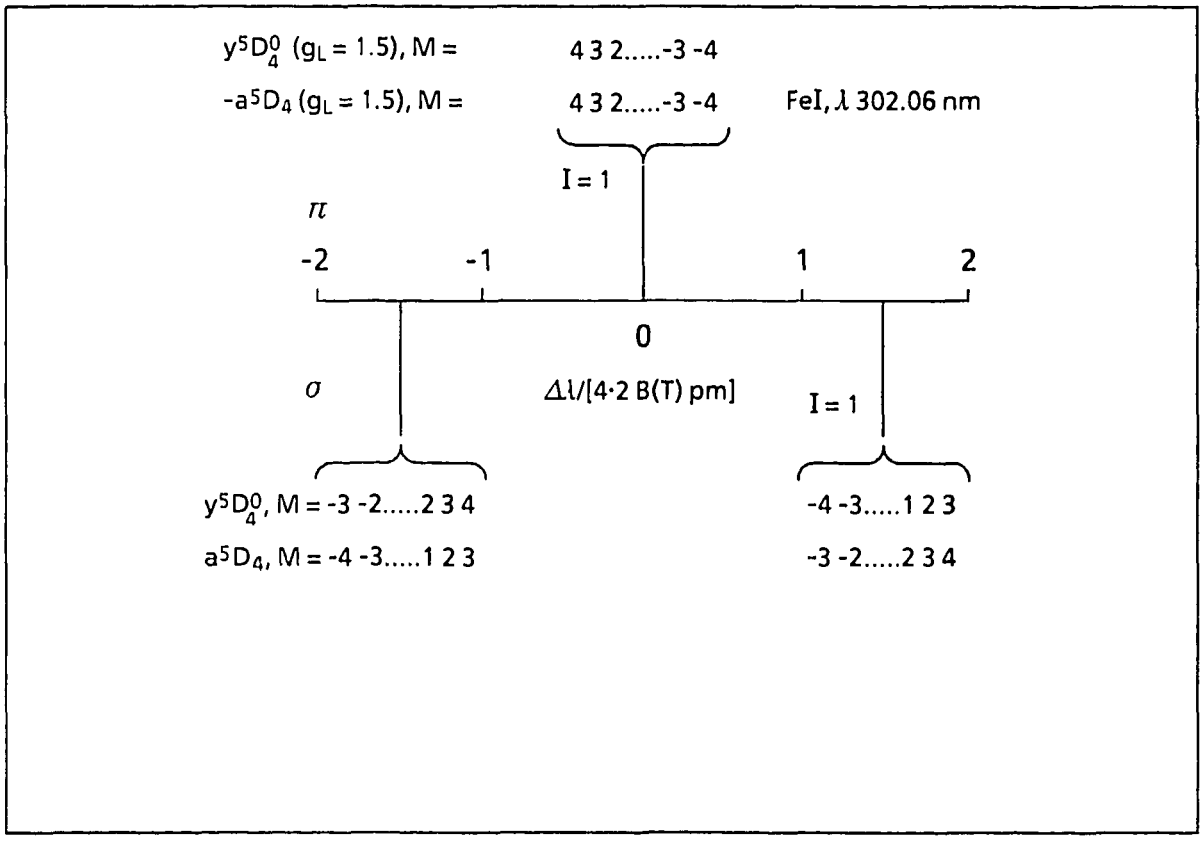

Fig.4 - Zeeman pattern for Fe I absorption line, λ=302.06 nm

therefore best to use π polarized laser light, for which the position of the centre of the absorption line component is independent of the magnetic field strength.

The Zeeman patterns of the nearby absorption lines mentioned in Sec. 4.1 are shown for a magnetic field of 10 T in Fig. 5.

For the fluorescence line at 382.04 nm between levels 2 and 3 the Zeeman pattern is more complex (Fig. 6). There are nine π and eighteen σ components. Their relative intensities may be calculated as indicated in Sec. 3.2 above, and the results are shown in the diagram. (When viewing the fluorescence at an angle of 90° to the magnetic field, the intensities given in the diagram for the σ component should be halved.) The unit of wavelength displacement is 6.82 pm per Tesla. The π polarized emission is contained in a much narrower bandwidth than the σ, so in the presence of noise due to continuum emission a better signal-to-noise ratio should be attainable with π. It will be seen that for B=10 T all the π components lie within ±34 pm. The π polarized detector filter bandwidth need therefore be no more than about 4×68~270 pm.

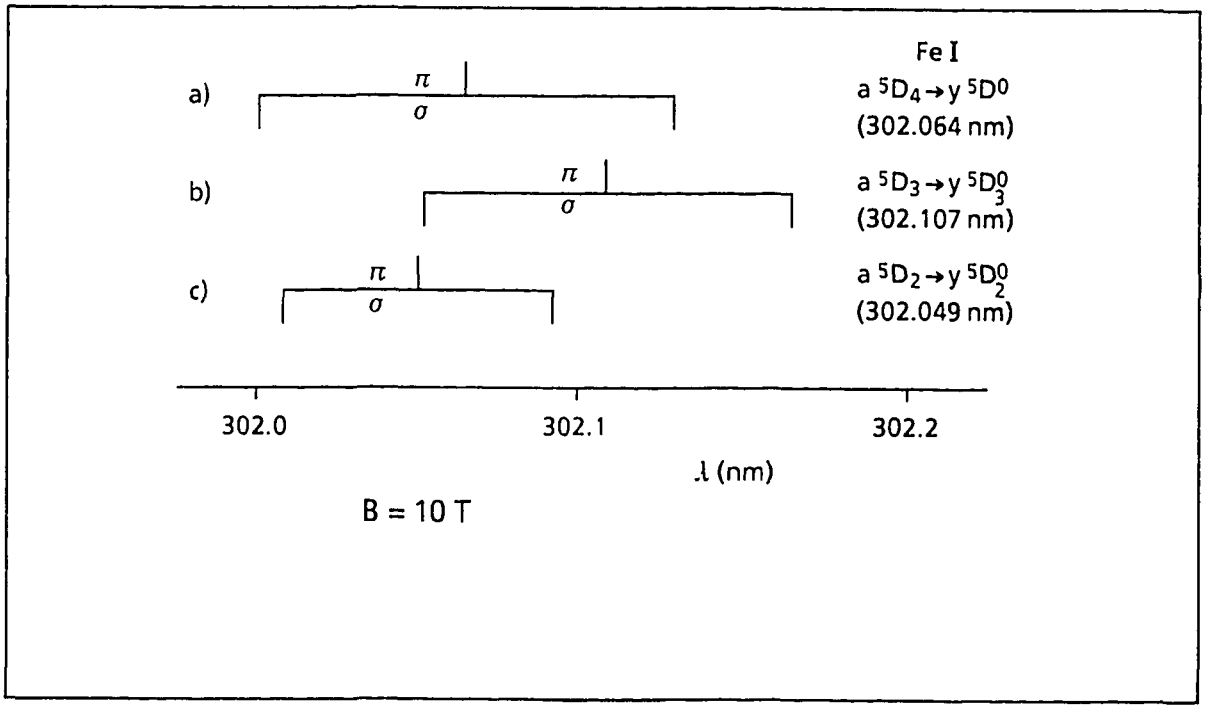

Fig.5 - Zeeman splittings at B=10 T for three adjacent Fe I lines

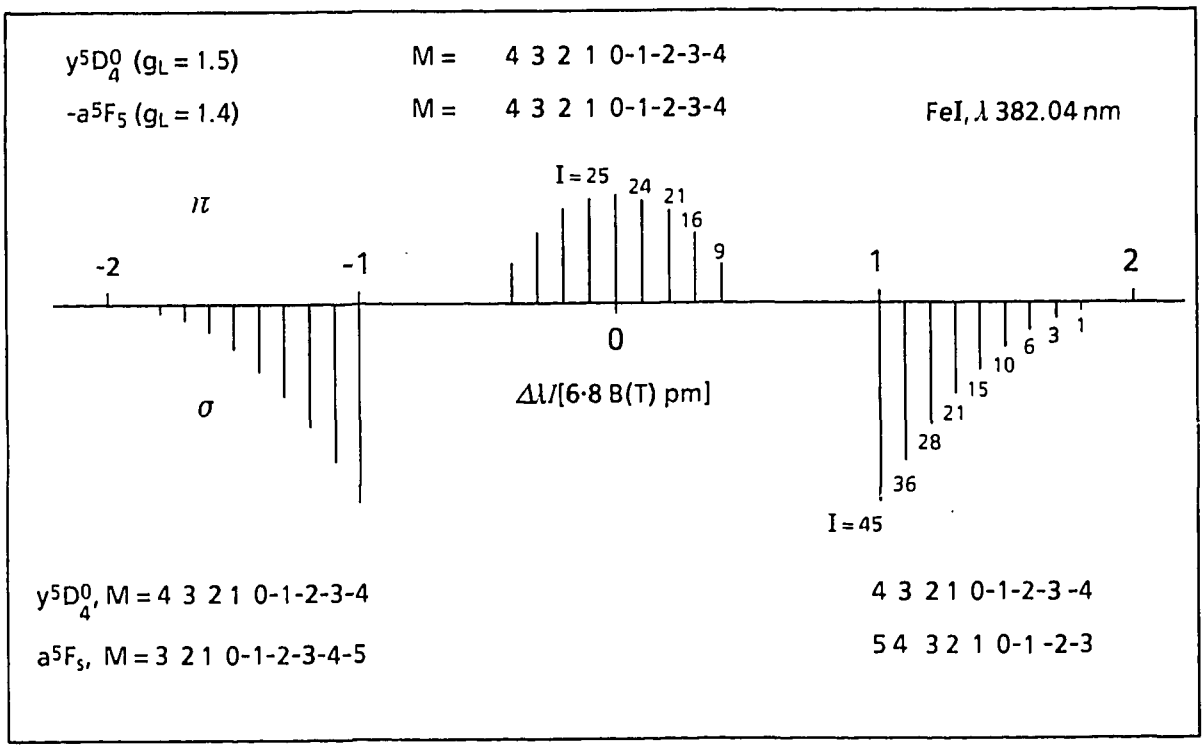

Fig.6 - Zeeman pattern for Fe I fluorescence line, λ=382.04 nm

4.3 - Fluorescence signal from the Fe I LIFS scheme in a magnetic field

When a laser with π polarization is used to excite an atom in a degenerate line such as the Fe I absorption line discussed above, then, if the laser bandwidth is broad compared to the absorption line profile, all atoms in all the nine magnetic states of the lower level will be pumped, and all the nine states of the upper level will be populated. If we assume for the moment a very short, intense laser pulse, which produces saturation in a time short compared to the lifetime of level 2, then at saturation, since $J_1=J_2$, the populations of all the upper states and all the lower states will be almost equal, so half the total number of atoms in level 1 in the interaction volume V will have been excited to the upper level. These will decay via several channels, including the fluorescence line of interest for LIFS which has a transition rate A_{23}. If the lifetime of the upper level is τ_2 and the total number density of Fe I atoms in the ground term is n_0, then (recalling the result of Sec. 4.1 for the population of the J=4 level) the total, time integrated number of fluorescence photons collected in π polarization in a detector solid angle $d\Omega$ is given by

$$N_F = \frac{0.57 n_0}{2} \frac{V d\Omega}{4\pi} \frac{A_{23}\tau_2}{3}. \tag{45}$$

This is similar to expression (21) of Sec. 2.2, but allows for the populations of the lower fine structure levels and the polarization of the emission. It assumes complete saturation and is thus an upper limit for a short pulse laser.

For a typical dye laser pulse with a duration of 10 ns the short pulse model is not appropriate, because τ_2 is only 5.9 ns (see Table I). A better estimate for the fluorescence yield in this case is obtained by assuming a finite constant laser pulse and using the results of Sec. 2.2 for $\tau_L/\tau \sim 2$: the same yield as the short pulse limit is then obtained with $S=5$, and the limiting yield for large S is twice this value. A full numerical calculation is of course needed for a real laser pulse shape (and it may be necessary to take into account repopulation of the ground state during the pulse) but we may expect that expression (45) for the short pulse limit also gives approximately the correct value of N_F for a 10 ns laser pulse with $S=5$, which from (12) corresponds to a laser irradiance per pm of bandwidth of 330 W cm^{-2}.

Introducing values of A_{23} and τ_2 from Table I we therefore find as a realistic estimate

$$N_F = 4.1 \times 10^{-2} n_0 \frac{V d\Omega}{4\pi}. \tag{46}$$

4.4 - LIFS Doppler measurements for Fe I atom velocities

The component of the velocity of an absorbing atom along the direction of the laser beam gives rise to a Doppler shift in the absorption line frequency.

Atoms with a thermal, Maxwellian velocity distribution have a Gaussian absorption line profile. In plasmas this is generally broad compared to the natural line width. The full width at half maximum intensity (FWHM) is given by

$$\frac{\Delta\lambda_D}{\lambda} = 7.162 \times 10^{-7}\left(\frac{T(K)}{A}\right)^{1/2} \tag{47}$$

where A is the atomic weight. Then, for example, for the iron absorption line at 302.06 nm, with A=56, when T=4000 K the FWHM of the Gaussian is

$$\Delta\lambda_D = 1.8 \text{ pm}.$$

The shift of the Gaussian for a flow velocity V is given by

$$\frac{\Delta\lambda_F}{\lambda} = \frac{V}{c}, \tag{48}$$

so for V=2 km s^{-1}, with λ=302.06 nm,

$$\Delta\lambda_F = 2.0 \; pm.$$

The velocity distributions of a number of different atoms sputtered from solid surfaces by various high energy ions have been measured by several authors using LIFS: this work has been well reviewed in Ref. [20]. In general, the velocity distributions normal to the surface rise from zero at V=0 to a maximum at V somewhere between 1 and 5 km s^{-1}, and then fall approximately exponentially at higher velocities. The FWHM of the distribution is typically 2 to 10 km s^{-1}. The distributions can be fitted by a formula due to Thompson [21]. Similar distributions may be expected in the edge plasma of a tokamak.

The wavelength displacements of interest are small compared to the separations of adjacent spectral lines in Fe I. Using a tunable laser with a narrow bandwidth of about 1 pm it is therefore possible to measure the Doppler profile and hence the velocity distribution of sputtered atoms by scanning the laser wavelength through the absorption line profile. The narrow laser bandwidth required can be achieved with a dye laser by inserting a mode-selecting etalon in the oscillator cavity. Because of the inhomogeneous Doppler broadening, only a fraction of the ground state atoms will be excited at a given setting of the laser wavelength, so the number of fluorescence photons collected per laser pulse will be smaller than that given for a broad band laser in expression (46). It is clearly important to avoid power broadening of the measured absorption line profile.

5 - LIFS CALCULATIONS FOR Mo I ATOMS

5.1 - Selection of LIFS transitions

Extensive measurements of lifetimes and transition probabilities have been reported by Whaling et al (Refs.[22, 23, 24] and private communication). A survey of absorption lines and subsequent fluorescence lines in Mo I has identified two feasible LIFS schemes. Both start from the ground level A^7S_3 (this term has no fine structure) as level 1. In Scheme (a), absorption excites the atom to $z^5P_3^0$, level 2(a), at a wavelength of 345.64 nm, and fluorescence is observed near 550.65 nm from the transition to a^5S_2 (level 3). In Scheme (b), absorption is to $z^5P_2^0$, level 2(b), at 346.68 nm, and fluorescence is observed near 553.30 nm, again to level 3. The large separation of the fine structure levels of the z^5P^0 term means that there will be no interference between the two schemes.

The transition rates and other atomic data for the two schemes are given in Table I. The absorption is stronger in Scheme (a) than in Scheme (b), and this is apparent in the larger values of S.

5.2 - The Zeeman effect in Mo I

The Landé factors for the various levels may be calculated from expression (35).

For level 1 in both schemes, J=3, L=0, S=3, and g_L=2; the experimental value [15] is 1.992.

For level 2(a), J=3, L=1, S=2, g_L=1.666 (experimental value 1.664).

For level 2(b), J=2, L=1, S=2, g_L=1.833 (experimental value 1.831).

For level 3, J=2, L=0, S=2, g_L=2 (experimental value 1.980).

The Zeeman patterns for the absorption lines have been calculated and are shown in Figs. 7 and 9. The total width, or spread, of the π polarized pattern in a field of 10 T is ± 56 pm for Scheme (a) (at 345.6 nm), and ±18 pm for Scheme (b) (at 346.7 nm).

For the fluorescence lines the patterns are shown in Figs. 8 and 10. The spreads of the π patterns at 10 T are ±93 pm for Scheme 9a) (near 550.6 nm) and ±47 pm for Scheme (b) (near 553.3 nm). The σ fluorescence patterns have spreads at 10 T of ±330 pm for Scheme (a) and ±310 pm for Scheme (b). These spreads should present no problems for the detection system with a filter bandwidth (FWHM) of 2 nm (or less at lower magnetic fields).

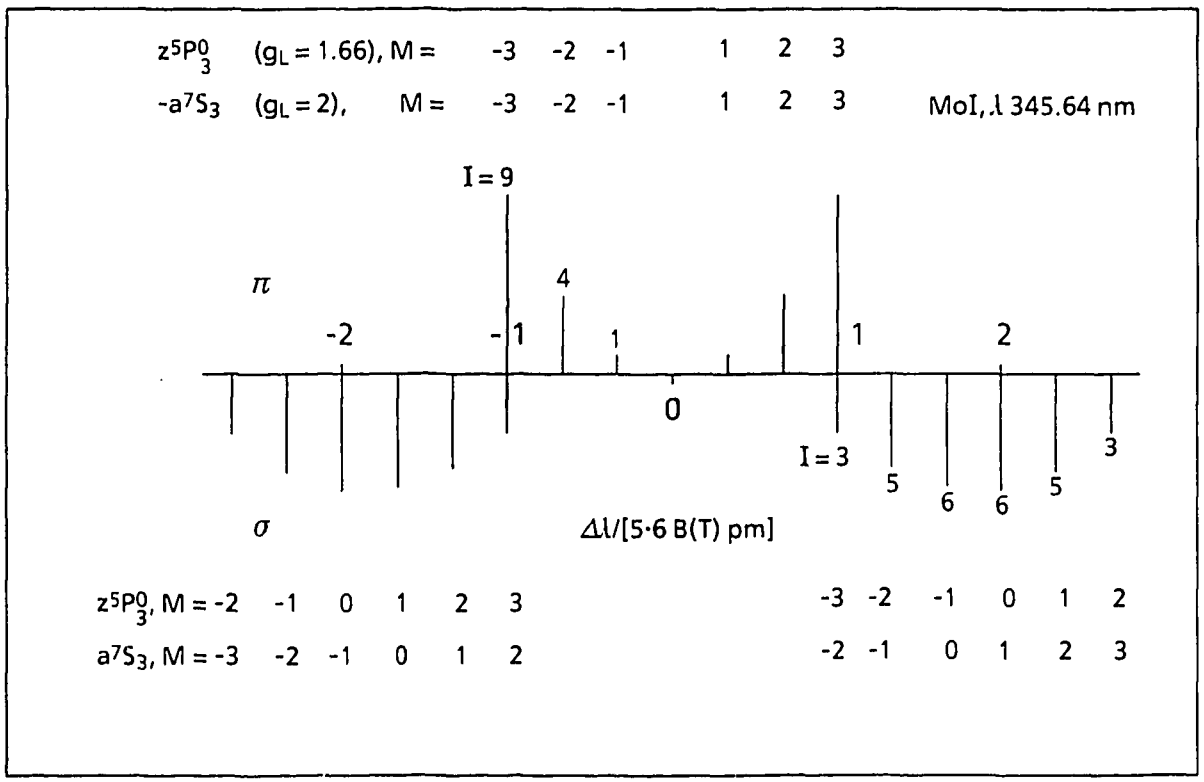

Fig.7 - Zeeman pattern for Mo I absorption line (Scheme (a)), λ=345.64 nm

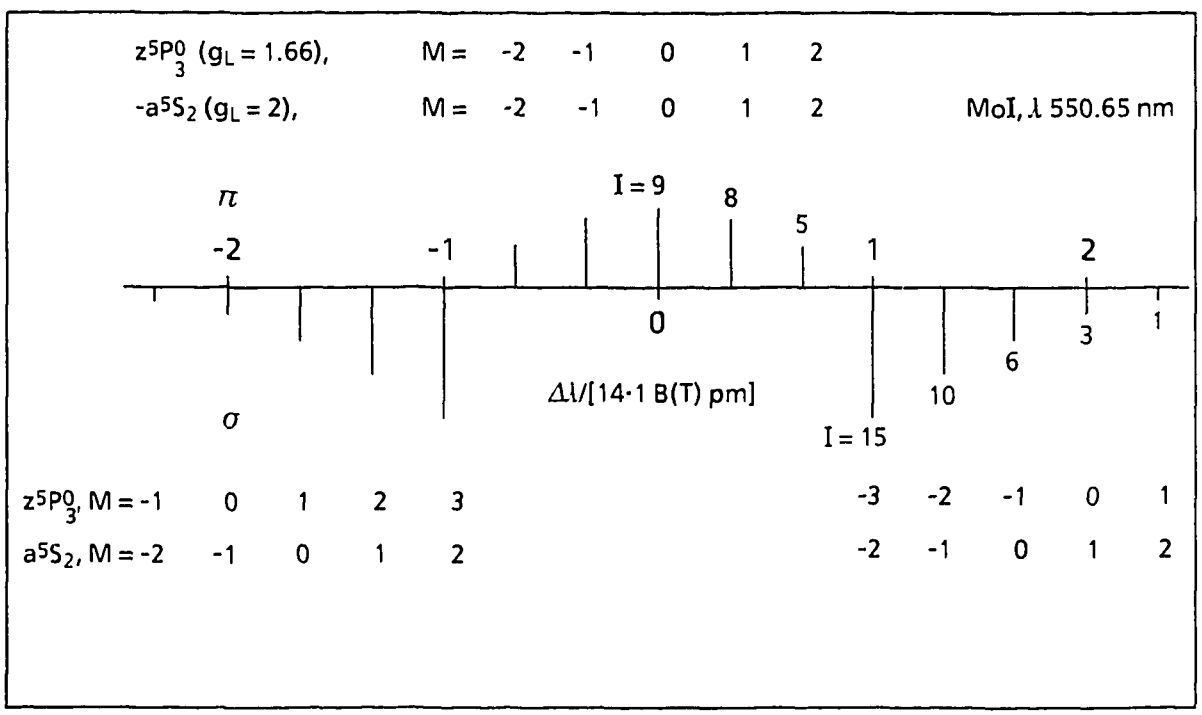

Fig.8 - Zeeman pattern for Mo I fluorescence line (Scheme (a)), λ=550.56 nm

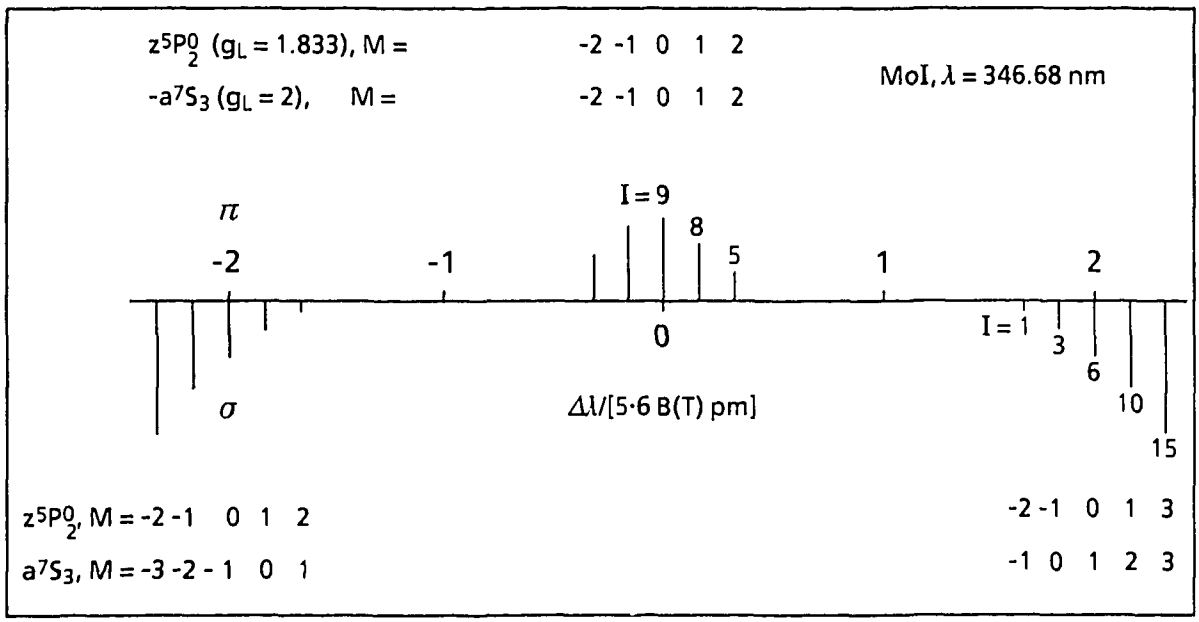

Fig.9 - Zeeman pattern for Mo I absorption line (Scheme (b)), λ=346.68 nm

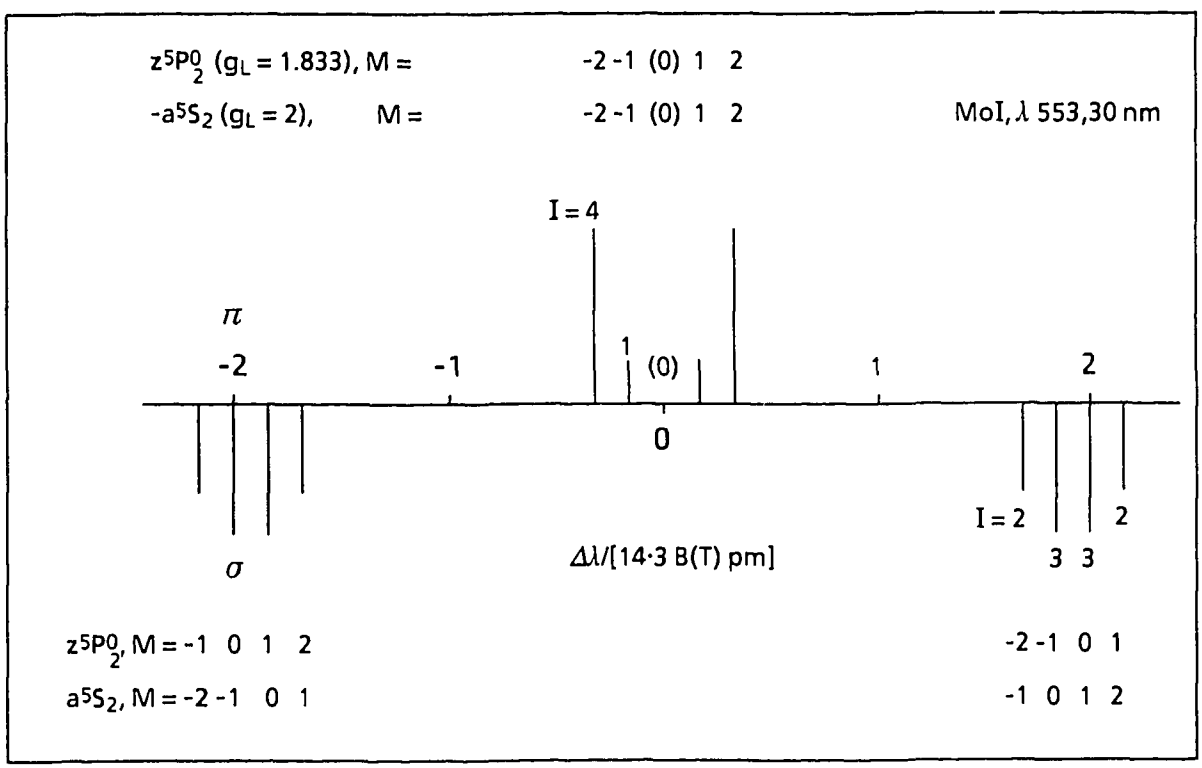

Fig.10 - Zeeman pattern for Mo I fluorescence line (Scheme (b)), λ=553.30 nm

In contrast to the Fe I case, where the π polarized absorption line has only a single component, the Mo I absorption is split into 5 or 6 Zeeman components separated by more than the usual laser bandwidth. The implications will be discussed below.

5.3 - Doppler effect for Mo I atoms

For the same conditions as were discussed in Sec. 4.3 for Fe I atoms, the FWHM of a Doppler broadened Mo I absorption line component near 346 nm at T=4000 K (with atomic number 96) is 1.6 pm. The wavelength shift for a flow speed of 2 km s^{-1} is 2.3 pm. These are small compared to the separation of the absorption line π components in a field of 10 T, which are 18 pm for Scheme (a) and 9 pm for Scheme (b). When the laser wavelength is scanned across the Zeeman pattern of the absorption line, each of the Zeeman components will be excited in turn, and each component will be affected by the Doppler broadening and shift. This effect is discussed further below.

5.4 - Optimising LIFS for Doppler measurements on Mo I atoms

If the absorption line Doppler profile of Mo I is to be measured in FTU, the Zeeman effect must be allowed for. This is in contrast tot he degenerate Fe I case discussed above, where if a π polarized laser is used the Zeeman effect can generally be ignored apart from the polarization dependence of the fluorescence intensity.

In Scheme (a) for Mo I if a π polarized laser is used and scanned over the wavelength range covering the entire π Zeeman pattern ($\pm$ about 60 pm at B=10 T, see Fig. 7) then each of the six non-zero Zeeman components will be scanned in turn, and the Doppler profile will affect each component. There is unfortunately no absorption at the unshifted wavelength in a magnetic field, and M_2=0 cannot be pumped in π polarization. Provided the magnetic field does not change during the scan, each of the absorption line components will have a similar Doppler modified profile, and the signal obtained by collecting the emission in all the fluorescence components will give each profile in turn. If, however, there is any significant variation in the local magnetic field over the emitting volume, or during the laser scan, then the spacing between the components of the Zeeman pattern will change proportionally to B and the Doppler profile deduced from the scan will be distorted. If a resolution of say 0.5 pm in the Doppler profile is required the permissible variation in B during the scan is only about 3% for the M=1 to 1 and -1 to -1, or 1% for the 3 to 3 and -3 to -3 transitions, which may not be attainable.

The relative intensities at 90° to $\underline{B}$ for all fluorescence transitions from each of the available level 2 magnetic states in Scheme (a), assuming equal populations, are (see Fig. 8):

	σ	π
M_2=±3	7.5	0
±2	5	5
±1	3.5	8

from a total for all directions of 105. The strongest fluorescence intensity will thus be obtained from the M_2=1 or -1 state with π polarized observation. However, much the strongest π Zeeman components of the 345.6 nm absorption line are M=3 to 3 and -3 to -3, displaced by ± 56 pm when B=10 T: the resulting fluorescence from the M_2=+3 or -3 state (Fig. 8), which will only be observed with σ polarization, displaced by ±141 pm, is only slightly weaker (7.5 compared with 8) than that from M_2=+1 or -1. Marginally better results will be obtained from the -3 to -3 absorption transition than from the 3 to 3, because of the small difference in the populations of the magnetic sublevels of level 1 due to the Boltzmann factor. We shall thus assume that in Scheme (a) we use the M=-3 to -3 π absorption component, and that we detect the fluorescence in σ polarization. The detector filter bandwidth should be no wider than is necessary to collect the fluorescence efficiently, because the plasma noise received by the detector (see Sec. 6) increases with the bandwidth. A FWHM of about four times the separation of the most widely displaced fluorescence components, i.e. 4×282 pm = 1.1 nm in this case, should be adequate for B up to 10 T.

Scheme (b) has the major advantage that the strongest component of the π polarized absorption (see Fig. 9) is due to the M=0 to 0 transition, whose wavelength is not Zeeman shifted. If the laser wavelength is scanned through this component the resulting Doppler profile should be unaffected by variations in B. Because there is no π polarized M=0 to 0 fluorescence (see Fig. 10), it is then necessary to observe the M=0 to ±1 transitions in σ polarized emission. These have almost the strongest fluorescence intensities at 90° to B. They are displaced by ±286 pm at 10 T, so a FWHM detector bandwidth of 2.3 nm should be adequate up to this magnetic field.

The foregoing considerations suggest that Scheme (b) is preferable to Scheme (a) for Doppler measurements on FTU, provided that the magnetic field is sufficiently strong for the separation between adjacent Zeeman components in the absorption line at 346.7 nm to be greater than the total breadth of the Doppler profile of interest, that is to say there is no significant overlap between the Doppler profiles on adjacent Zeeman components. If we use the criterion that the spacing between absorption line Zeeman components must be greater than twice the FWHM of the Gaussian profile due to a temperature T, this implies

{Scheme (b)} $T(K)<340\ B^2$.

With B=10 Tesla, therefore, Doppler profiles for temperatures up to 34,000 K (3 eV) could be measured. A general Doppler shift due to a flow velocity would apply equally to all components and would not lead to overlap. There might however be some ambiguity if the

entire pattern was not observed, unless the shift was less than the spacing between Zeeman components, i.e. unless

{Scheme (b)} $V<0.8$ B km s^{-1}.

In Scheme (a) similar constraints would apply, but would be less severe because of the larger separation of the components:

{Scheme (a)} $T(K)<1350\ B^2$,

{Scheme (b)} $V<1.6$ B km s^{-1}.

Scheme (a) might therefore be preferable at very high temperatures or using low magnetic fields.

5.5 - *Fluorescence intensities from the Mo I LIFS schemes in a magnetic field with no resolution of the Doppler profile*

When a sufficiently narrow band laser with π or σ polarization is used to excite a line with a non-degenerate Zeeman pattern in a magnetic field, only one of the Zeeman components of level 2 can be excited at a time. The Zeeman splitting is generally small enough for the initial populations of the magnetic states of the lower level to be assumed to be almost equal. Thus if the laser pulse is short compared to the relaxation time of the populations, then even with very high power only $1/(2J_1+1)$ of the lower level 1 atoms will be pumped to level 2. This may considerably reduce the fluorescence signal as compared to the case of a line with a degenerate Zeeman pattern. We shall now estimate the fluorescence intensities for the two Mo I schemes, for short, high power π polarized laser pulses whose bandwidth in each case covers the full Doppler profile of a single Zeeman component of the absorption line. For a real laser pulse profile a more detailed calculation is necessary: the results of Sec. 2.2 for a constant power laser pulse indicate that with $\frac{t_L}{t_2} \sim 0.5$ the photon yield will be increased to perhaps 1.3 times the short pulse limit.

It should be noted that when only one of the level 2 states is excited, the spontaneous lifetime of the excited state will depend on the sum of the rates of all allowed transitions *from that state*. This may be significantly different from the normal averaged lifetime of the upper level, and should be calculated. For the present, we have avoided this problem and assumed that each state of level 2 has the same lifetime τ_2.

Mo I Scheme (a)

The relative intensities of the fluorescence line components shown in Fig. 8 were calculated, as usual, assuming equal numbers of atoms in each of the $(2J_2+1)$ magnetic states of level 2.

When added for all components they total 105. Thus a relative intensity of 7.5 for the σ components from M_2=3 or -3 at 90° to $\underline{B}$ implies that 7.5/105 of the total fluorescence transition rate A_{23} per atom from level 2 would be observed, if the magnetic states were equally populated. However, we have chosen to populate only one of the magnetic states, so we should multiply this observable transition rate per atom by $2J_2$+1.

The narrow bandwidth laser excites only 1/($2J_1$+1) of the n_0 ground term atoms per unit volume, and at saturation only half of these will be pumped to level 2. Then the maximum possible number of fluorescence photons received, at full saturation, will be

$$N_F = \frac{n_0}{2(2J_1+1)} A_{23}\tau_2(2J_2+1)\frac{Vd\Omega}{4\pi}\frac{7.5}{105} \tag{49}$$

$$= \frac{7.5n_0}{210}\frac{Vd\Omega}{4\pi}A_{23}\tau_2. \tag{50}$$

Using values from Table I for A_{23} and τ_2, and assuming only half the saturation population of level 2, we find

$$N_F = 1.3\times10^{-2}n_0\frac{Vd\Omega}{4\pi}. \tag{51}$$

Mo I Scheme (b)

The maximum possible number of photons detected for these conditions is given, following a similar argument as for Scheme (a), by

$$N_F = \frac{n_0}{2(2J_1+1)} A_{23}\tau_2(2J_2+1)\frac{Vd\Omega}{4\pi}\frac{3}{30} \tag{52}$$

$$= \frac{n_0}{28}\frac{Vd\Omega}{4\pi}A_{23}\tau_2. \tag{53}$$

Introducing values of A_{23} and τ_2,from Table I, and again assuming only half the saturation population of level 2, we find for Scheme (b)

$$N_F = 1.3\times10^{-2}n_0\frac{Vd\Omega}{4\pi} \tag{54}$$

which is coincidentally the same as expression (51) for Scheme (a).

It should be emphasised that expressions (49) and (53) both assume that the laser bandwidth is sufficiently wide to cover the entire Doppler profile of an individual Zeeman component.

6 - APPLICATIONS OF LIFS TO FTU

We shall now make use of the foregoing results to estimate the performance of LIFS as applied to FTU.

We shall assume that sufficient laser power is available to approach saturation without causing unacceptable power broadening of the absorption transition. The choice of laser dye and solvent are crucial for satisfactory operation at a given wavelength, but Borra's experiments on power broadening, together with recent experiments at ENEA on laser dyes and solutions indicate that adequate laser power should be available from the existing excimer-laser pumped dye laser.

6.1 - Minimum Fe I and Mo I densities for LIFS measurements on FTU with no resolution of the Doppler profile

The geometry of the diagnostic optics on FTU will be assumed to be that given in Ref. [9]. The essentially parallel laser beam enters the FTU torus perpendicularly to $\underline{B}$ through a window and an aperture in the limiter with an area of 10^{-4} m^2. Fluorescence emitted in the opposite direction is observed through the same window. The thickness of the edge plasma layer from which Fe I radiation is emitted has been estimated to be 10^{-3} m: we shall assume a similar thickness for Mo I. (This may be a low value: in Textor, it was found that the density of Fe I atoms fell off exponentially with distance from the limiter surface, with a characteristic length of 6.5 mm [4].) Thus the emitting volume $V=10^{-7}$ m^3. The fluorescence is collected by a lens whose aperture is such that $d\Omega/4\pi=7\times10^{-5}$, so $Vd\Omega/4\pi=7\times10^{-12}$ m^{-3}. If the fluorescence is detected, after filtering, by a photomultiplier, we may estimate the approximate number of photoelectrons produced, N_p, to be $N_F/50$ (we assume the same efficiency for all the fluorescence wavelengths). Then

for Fe, $\quad N_p=5.7\times10^{-15}\, n_0$

for Mo, $\quad N_p=1.8\times10^{-15}\, n_0$

Bremsstrahlung, together with stronger quasi-continuum emission from the cool edge regions, are expected to be the main sources of noise from the plasma. Further experimental work is needed to determine the plasma noise level accurately for the actual line of sight and the plasma conditions to be used for LIFS, but measurements by McNeill et al. (private communication) indicate that a typical photon flux collected by a detector looking across a diameter of the FTU plasma is about 2×10^{16} photons m^{-2} sterad^{-1} s^{-1} mm^{-1} at wavelengths near 540 nm. Near 380 nm this is increased by a factor of 1.4. Emission at the fluorescence wavelengths due to collisional excitation is expected to be small [9]. Thus for the conditions

assumed here, and using a 10 nm filter bandwidth, calculations similar to those given in Ref. [9] indicate that the number N_B of photoelectrons detected due to the plasma noise during an integration time of 100 ns at 380 nm, near the Fe I fluorescence wavelength, is 49, while in the region of 540 nm (the Mo I fluorescence wavelength) N_B=35.

The signal-to-noise ratio (*S/N*) is then given by

$$S/N = \frac{N_p}{\sqrt{N_p + N_B}}. \tag{56}$$

To obtain a *S/N* of 10, then

$$\text{for Fe I,} \quad N_p = 136, \quad \text{and } N_0 = 2.4\times10^{16}\ \text{m}^{-3}$$

$$\text{while for Mo I,} \quad N_p = 127, \quad \text{and } N_0 = 7\times10^{16}\ \text{m}^{-3} \tag{57}$$

These results are for complete absorption components, with no attempt to measure the Doppler profile. The detection limits, defined as the densities of atoms which gives *S/N*=2, require

$$\text{for Fe I,} \quad N_p = 16, \quad \text{so } N_0 = 2.8\times10^{15}\ \text{m}^{-3}$$

$$\text{while for Mo I,} \quad N_p = 14, \quad \text{and } N_0 = 7.8\times10^{15}\ \text{m}^{-3}. \tag{58}$$

If the laser bandwidth is narrower than the Doppler broadened absorption line (or component) there will be some loss of signal because all the atoms in the lower state will not be pumped. In this case these density limits will be increased. On the other hand, the density limits given in (57) and (58) could be lower if the detector filter bandwidth was reduced to say 2 nm, thereby reducing the number of plasma noise photoelectrons detected during 10^{-7} s to N_B=10 for Fe I and 7 for Mo I. The results are summarised below:

		S/N=2	*S/N*=10
10 nm filter			
	n_0 (Fe I)	2.8×10^{15} m^{-3}	24×10^{15} m^{-3}
	n_0 (Mo I)	7.8	70
2 nm filter			
	n_0 (Fe I)	1.5	19
	n_0 (Mo I)	4.5	60

These results are for a single laser pulse. Averaging over n pulses will reduce the density limits, dividing them by a factor of $\sqrt{n}$. We may conclude, in broad agreement with Borra [9], that it should be possible to observe LIFS from the expected density of Fe I. It will be more difficult, by a factor of about 3 in density, to observe LIFS from Mo I in the edge plasma of FTU with the proposed optical system. A larger étendue of the collecting lens would improve the accuracy of the measurements.

6.2 - Minimum densities for LIFS Doppler profile measurements on FTU

If the Doppler profile is to be measured in some detail, at say 10 points, then the laser must be tunable over the profile and the laser bandwidth should be considerably narrower than the width of a single absorption component. Only that fraction of the atoms whose velocities bring their Doppler shifted absorption line wavelength within the narrow laser bandwidth will be excited. We must therefore reduce the values given in (55) for the ratio of N_p to the total number of ground term atoms, n_0, perhaps by a factor of 10. Then for S/N=10, using a 2 nm filter bandwidth, we find from (56)

$$\text{for Fe I,} \quad N_p = 109, \qquad \text{and } N_0 = 1.9\times10^{17}\ \text{m}^{-3}$$

$$\text{while for Mo I,} \quad N_p = 106, \qquad \text{and } N_0 = 6\times10^{17}\ \text{m}^{-3}, \tag{59}$$

assuming only a single laser pulse is used for each point measured during the scan of the absorption line profile.

These densities are rather higher than those we expect to find in FTU. The problem is primarily due to the small fluorescence signal, rather than the plasma noise, so reducing the filter bandwidth further will not have much effect. Three improvements can be considered.

(a) The emitting region could be enlarged by expanding the laser beam. Doubling the beam diameter will quadruple the signal.

(b) Reducing the required signal to noise to say 5 instead of 10 will help considerably.

(c) The signal could be averaged over say 10 laser pulses for each point on the scan of the absorption line profile

These changes will increase N_p/N_0 by a factor of 40, and the noise by a similar factor. Then for a S/N of 5, we find

$$\text{for Fe I,} \quad N_p = 113, \qquad \text{and } N_0 = 5\times10^{15}\ \text{m}^{-3}$$

$$\text{while for Mo I,} \quad N_p = 97, \qquad \text{and } N_0 = 1.3\times10^{16}\ \text{m}^{-3}. \tag{60}$$

These densities are not very different from the expected values in the FTU edge plasma, which are themselves uncertain. The prospects for being able to make velocity measurements, even

with the modified geometry optics and averaging over 10 laser pulses, are thus not yet clear, and can only be decided by experimental tests. If the results are not satisfactory there may nevertheless be considerable scope for improvement in the collection optics: if the étendue of the lens could be increased by a factor of 10 the density limits would be reduced by the same factor.

7 - CONCLUSIONS

The theory of LIFS is well understood and adequately confirmed by experimental results. The effects of laser pulse duration, of absorption and laser spectral line profiles, and of power broadening have been discussed in detail. Further experimental tests on power broadening are probably the only reliable way to determine the greatest acceptable laser irradiance in a given situation: much useful information can be obtained from simple sputtering discharges in the laboratory.

Satisfactory absorption and fluorescence transitions exist in both Fe I and Mo I for LIFS using an excimer laser pumped dye laser. The relevant wavelengths, transition rates and other atomic data are accurately known for both atoms. More detailed calculations of *effective* lifetimes of the upper magnetic sublevels are however needed, taking into account that, when only one Zeeman component absorbs laser light, the lifetime of the upper state is not the normal averaged spontaneous lifetime of the upper level as a whole.

The Zeeman effect is important for LIFS in the strong magnetic fields used in FTU. Detailed analyses of the low field Zeeman patterns for LS coupling have been presented for one scheme in Fe I and for two schemes in Mo I. It is found that in each case the Zeeman splitting is large compared with the expected Doppler broadening of the emission line profiles. Polarization effects have been considered in detail and the most suitable Zeeman components have been identified for each scheme. In the Fe I scheme the degeneracy of the absorption line simplifies LIFS calculations considerably: the Zeeman effect may be disregarded provided π polarized light is used: it is preferable to collect π polarized fluorescence.

In Mo I the Zeeman splittings in FTU magnetic fields will generally be large compared to the normal dye laser line widths and only a single Zeeman component can absorb laser light at a time. One scheme (Scheme (b)) is generally preferable to the other because there is an unshifted π polarized Zeeman component in the absorption line, which is unaffected by variations in the local magnetic field. However, the Zeeman splitting is greater in Scheme (a), and this may be helpful for LIFS at low magnetic fields or high temperatures of the absorbing atoms.

The observed polarization of the fluorescence emission is determined only by the direction of observation relative to the local magnetic field. The fluorescence photon yields have been calculated approximately for the selected transitions, taking into account the Zeeman structure and alsc, in the case of Fe I, the Boltzmann distribution of relative populations in the fine structure levels of the ground term.

Estimates of the expected plasma noise, based on spectroscopic measurements [7,8,] have been used to determine the minimum Fe I or Mo I atom densities for specified signal-to-noise ratios, assuming that the optical system described in Ref. [9] is employed on FTU. It is found that whereas the density of Fe I or Mo I should be measurable without too much difficulty, perhaps from a single laser pulse, it will probably be necessary to modify the optical arrangements and average over several laser pulses in order to determine the Doppler profiles and hence the velocity distributions of the absorbing atoms. Increasing the étendue of the lens collecting the fluorescence will improve the accuracy of the measurements.

8 - ACKNOWLEDGEMENTS

The work described in this report was begun during the author's visit to ENEA, Frascati during May and June 1993. He is greatly indebted to many people at ENEA for generous help and advice, especially Dr. Gerardo Gatti, Dr. Francesco Orsitto and Signora Maria-Rita Novelli. He is grateful to ENEA for support under Contract No. 93/58/45/AA, and to EURATOM for a mobility agreement arranged through the Culham Laboratory of AEA Technology. Dr. Beatrix Schunke (JET) kindly read the draft of the report and made many helpful comments.

9 - REFERENCES

[1] Muraoka, K. and Maeda, M., Pl. Phys. and Contr. Fusion **35**, 633 (1993).
[2] Schweer, H.B., KFA Julich Report No. 1876, 1983.
[3] Oda, T. et al., J. Nucl. Mater. **128-129**, 262 (1984).
[4] Bay, H.L. and Schweer, B., J. Nucl. Mater. **111 -112**, 732 (1984).
[5] Dullni, E., Dissertation (Bochum), KFA Julich Report No. 1936, 1984.
[6] Bessenrodt-Weberpals, M. et al., J. Nucl. Mater. **162-164**, 435 (1989).
[7] Condrea, I., Bartiromo, R., Mazzitelli, G. and McNeill, D.H., EPS Conference, Innsbruck, 1992.
[8] McNeill, D.H., EPS Conference, Innsbruck, 1992.
[9] Borra, M. Tesi di Laurea, II^{o} University, Rome.
[10] Yariv, A., *Quantum Electronics*, 2nd edition, J. Wiley (New York) 1975.
[11] Citron, M.L., Gray, H.R. Gabel, C.W. and Stroud, C.R., Phys. Rev. **A16**, 1507 (1977).
[12] Bogen, P. and Hintz, E.,in *Physics of Plasma Wall Interactions in Controlled Fusion*, Ed. D.E. Post and R. Behrisch, Plenum, 1986.
[13] Wright, R.B. et al., Surface Science **110**, 151 (1981).
[14] Wright, R.B. et al., Nucl. Instrum. Methods **182-183**, 167 (1981).
[15] Moore, C.E., Atomic Energy Levels, NBS Circular 467, 1952.
[16] Corney, A., Atomic and Laser Spectroscopy, Oxford University Press, 1977.
[17] O'Brian, T.R. et al., JOSA, **B8**, 1185 (1991).
[18] Elbern, A., Applied Phys. **15**, 111 (1978).
[19] Schweer, H.B. and Bay, H.L., Appl. Phys. **A29**, 53 (1982).
[20] Bay, H.L., Nucl. Instrum. Methods **B18**, 430 (1987).
[21] Thompson, M.W. Phil. Mag. **18**, 377 (1968).
[22] Whaling, W. et al., J. Quant. Spectr. Rad. Transfer **32**, 69 (1984).
[23] Whaling, W. et al., J. Quant. Spectr. Rad. Transfer **36**, 491 (1986).
[24] Whaling and Brault, J.W., Physica Scripta 38, 707 (1988).